AD-A070 016 MARYLAND UNIV COLLEGE PARK DEPT OF PHYSICS AND ASTRONOMY F/G 20/2
INVESTIGATION OF NOISE IN SOLIDS AT LOW TEMPERATURES.(U)
APR 79 W S DAVIS, H J PAIK, J - RICHARD F49620-77-C-0065
UNCLASSIFIED AFOSR-TR-79-0693 NL

| OF |
AD
A070016

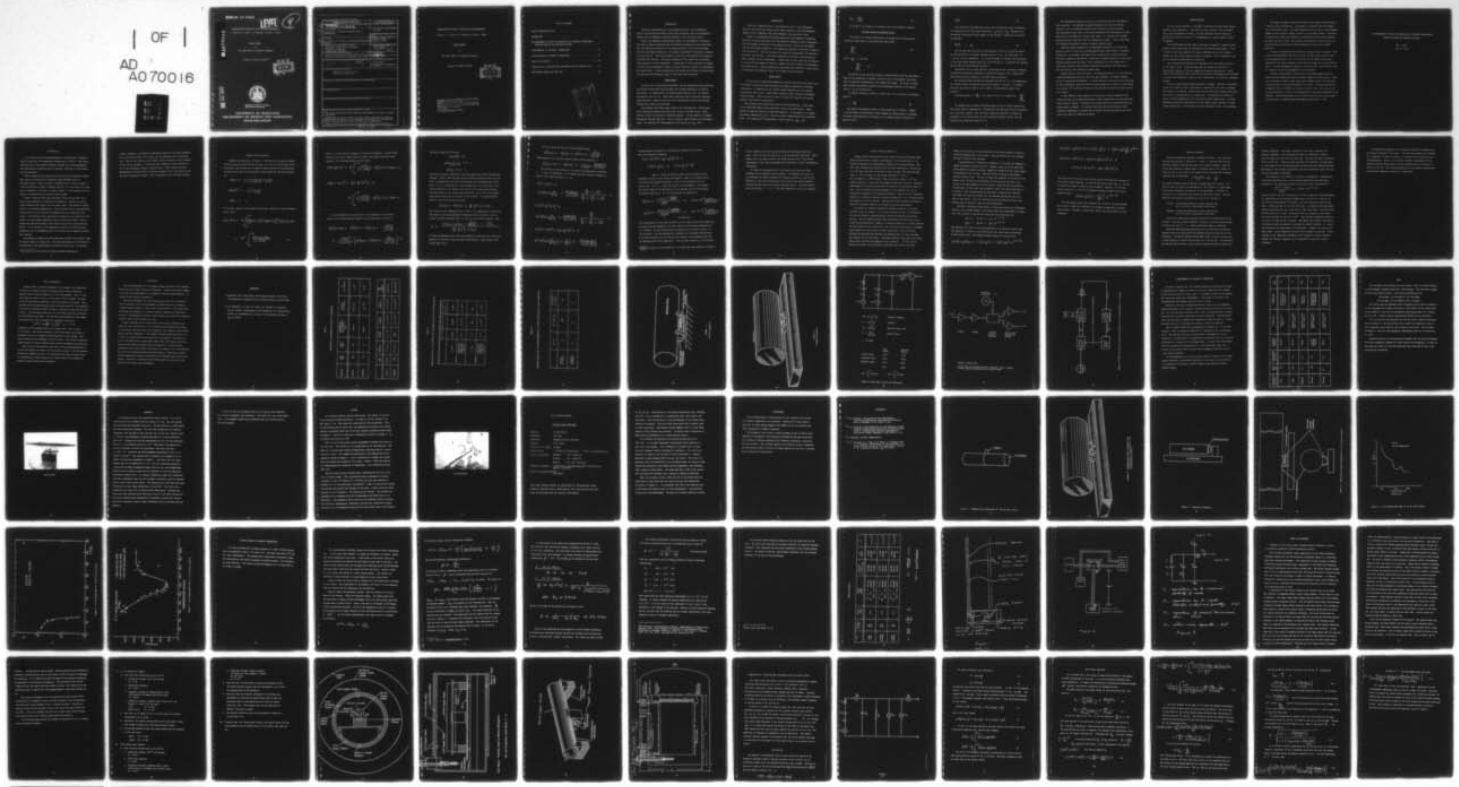

END
DATE
FILMED
7-79
DDC

LEVEL II

4

INVESTIGATION OF NOISE IN SOLIDS AT LOW TEMPERATURES

W. Davis, H. J. Paik, J.-P. Richard, K. Krack, J. Weber

ANNUAL REPORT

to

AIR FORCE OFFICE OF SCIENTIFIC RESEARCH

Contract F 49620-77-C-0065

UNIVERSITY OF MARYLAND
DEPARTMENT OF PHYSICS AND ASTRONOMY
COLLEGE PARK, MARYLAND

SECURITY CLASSIFICATION OF THIS PAGE (When Data Entered)

REPORT DOCUMENTATION PAGE	READ INSTRUCTIONS BEFORE COMPLETING FORM
1. REPORT NUMBER (18) (19) AFOSR-TR-79-0693	2. GOVT ACCESSION NO. / 3. RECIPIENT'S CATALOG NUMBER
4. TITLE (and Subtitle) (6) INVESTIGATION OF NOISE IN SOLIDS AT LOW TEMPERATURES.	5. TYPE OF REPORT & PERIOD COVERED: Interim
	6. PERFORMING ORG. REPORT NUMBER (15)
7. AUTHOR(s) (10) Wm. S. Davis, H. J. Paik, J.-P. Richard, K. Krack J. Weber	8. CONTRACT OR GRANT NUMBER(s): F 49620-77-C-0065
9. PERFORMING ORGANIZATION NAME AND ADDRESS: Department of Physics and Astronomy, University of Maryland, College Park, MD 20742	10. PROGRAM ELEMENT, PROJECT, TASK AREA & WORK UNIT NUMBERS: 61102F 2301/A1 (16) (17) A1
11. CONTROLLING OFFICE NAME AND ADDRESS: Air Force Office of Scientific Research /NP (11), Bolling Air Force Base, Washington, D.C. 20332	12. REPORT DATE: April 1979
	13. NUMBER OF PAGES: 79
14. MONITORING AGENCY NAME & ADDRESS (if different from Controlling Office): (9) Annual rept., (12) 82p.	15. SECURITY CLASS. (of this report): Unclassified
	15a. DECLASSIFICATION/DOWNGRADING SCHEDULE

16. DISTRIBUTION STATEMENT (of this Report)

Approved for public release;
distribution unlimited.

17. DISTRIBUTION STATEMENT (of the abstract entered in Block 20, if different from Report)

18. SUPPLEMENTARY NOTES

19. KEY WORDS (Continue on reverse side if necessary and identify by block number)

20. ABSTRACT (Continue on reverse side if necessary and identify by block number)

The theory of the noise which limits the measurements of strains in solids is presented.

Measurements of quality factors of nearly perfect crystals are summarized together with the status of the development of procedures for observing the noise of very high quality factor crystals at low temperatures.

Design calculations for a large 20 millikelvin cryostat are presented.

DD FORM 1473

219 638 LB

INVESTIGATION OF NOISE IN SOLIDS AT LOW TEMPERATURES

W. Davis, H. J. Paik, J.-P. Richard, K. Krack, J. Weber

ANNUAL REPORT

to

Air Force Office of Scientific Research

Contract F 49620-77-C-0065

TABLE OF CONTENTS

INTRODUCTION

Electrical communications at room temperature have a noise background which is associated with thermal (black body) radiation, other electromagnetic signals such as lightning, switching transients, and electronics noise.

Nearly all geophysical measurements employ an electromagnetic transducer. The noise is partly associated with the amplifier-transducer, partly associated with the thermal fluctuations of the measuring device, and partly associated with the environment background. For example a gravimeter is employed to measure earth surface "g". Such an instrument is usually an accelerometer with appropriate sensor and recorder. Some noise originates in the sensor and electronics, some originates in the accelerometer. Usually most of this noise has its origins in local earth disturbances[1] related to seismic activity, weather, the atmosphere, and ocean effects. Gravity gradiometers have sensitivity limited by various kinds of electrical and mechanical noise, in the sensor and electronics.

Noise Limits

If there were no significant background, and the electronics were noise free, the thermal fluctuations would determine the ultimate background of existing instruments. As temperatures are lowered towards absolute zero, the thermal fluctuations tend to zero. Under these conditions other fluctuation phenomena become apparent. These are the zero point fluctuations in matter and certain quantum noise limits in electronics.

The ultimate electronics noise arises in the following way. Linear electronic amplifiers employ either electrons or ions in excited states. These amplify through the process of stimulated emission. In the absence of a signal, spontaneous emission may occur. This is a purely random process and contributes noise. The temperature[2] corresponding to this process is T_{QN}, with

INTRODUCTION

Electrical communications at room temperature have a noise background which is associated with thermal (black body) radiation, other electromagnetic signals such as lightning, switching transients, and electronics noise.

Nearly all geophysical measurements employ an electromagnetic transducer. The noise is partly associated with the amplifier-transducer, partly associated with the thermal fluctuations of the measuring device, and partly associated with the environment background. For example a gravimeter is employed to measure earth surface "g". Such an instrument is usually an accelerometer with appropriate sensor and recorder. Some noise originates in the sensor and electronics, some originates in the accelerometer. Usually most of this noise has its origins in local earth disturbances[1] related to seismic activity, weather, the atmosphere, and ocean effects. Gravity gradiometers have sensitivity limited by various kinds of electrical and mechanical noise, in the sensor and electronics.

Noise Limits

If there were no significant background, and the electronics were noise free, the thermal fluctuations would determine the ultimate background of existing instruments. As temperatures are lowered towards absolute zero, the thermal fluctuations tend to zero. Under these conditions other fluctuation phenomena become apparent. These are the zero point fluctuations in matter and certain quantum noise limits in electronics.

The ultimate electronics noise arises in the following way. Linear electronic amplifiers employ either electrons or ions in excited states. These amplify through the process of stimulated emission. In the absence of a signal, spontaneous emission may occur. This is a purely random process and contributes noise. The temperature[2] corresponding to this process is T_{QN}, with

$$T_{QN} = \frac{\hbar\omega}{k \ln_e 2} \qquad (1)$$

In (1) $\hbar\omega$ is the energy of one quantum, and k is Boltzmann's constant.

Intrinsic Noise of An Elastic Solid

If a solid is in thermal equilibrium, the equipartition theorem states that each normal mode of oscillation will have energy.

$$\frac{\hbar\omega}{e^{\frac{\hbar\omega}{kT}}-1} \qquad (2)$$

and if $\frac{\hbar\omega}{kT} << 1$, we have

$$\frac{\hbar\omega}{e^{\frac{\hbar\omega}{kT}}-1} \simeq kT$$

In practice we are observing strains or displacements caused by some effect which we are attempting to measure, and the strain or displacement fluctuates with an amplitude corresponding to the normal mode energy. The extent to which these thermal fluctuations interfere with measurements depends on the quality factor Q, in the following way.

For angular frequency ω there is a decay time τ for a transient disturbance, given by

$$\tau = \frac{2Q}{\omega} \qquad (3)$$

The energy fluctuations consist of noise wavetrains of duration roughly τ seconds before the amplitude or phase changes by a large amount, on average. If we make some observation of duration Δt the thermal energy fluctuation is expected to be[3]

$$\frac{kT\,\Delta t}{\tau} \qquad (4)$$

With electronic instrumentation there will be additional noise contributed by the amplifier with some noise temperature T_N with $T_N > T_{NQ}$ defined by (1). The minimum "detectable energy change" at the resonance frequency of the solid is therefore

$$\frac{kT\,\Delta t}{\tau} + kT_N \qquad (5)$$

One can show that this equation holds within a factor of 2 when the motion is observed below its resonance frequency with $\Delta t \cong \pi/\omega$. The quantities Δt, τ, and T_N are not independent. For a given strength of coupling the electronics to the system being observed there will be an optimal Δt. Increasing the coupling may decrease the Q and thereby decrease τ.

Nonetheless (5) is a good guide for indicating how the technology to measure accelerations and gravity gradients is improved by going to lower temperatures, higher quality factor materials, and lower noise electronics.

All presently known systems are described very well by (5). As temperatures are lowered further and quality factors also improve, eventually (5) becomes less than one phonon or photon, and a number of modifications appear to be required.

As already noted, if $\frac{\hbar\omega}{kT}$ is not small, kT in (5) is replaced by $\frac{\hbar\omega}{e^{\frac{\hbar\omega}{kT}}-1}$

(5) assumes that a system is employed which is kept in thermal equilibrium with a heat bath at temperature T. Historically this has been the most convenient way to operate a system. Also the linear electronic amplifiers invented and developed in this century have all been stimulated emission devices with the limiting noise temperature given by (1).

The measurement problem can be set up in different ways not described by these equations. For example, the quantum mechanics tells us that certain quantities can in principle be measured with arbitrarily great precision. Such measurements then limit the precision obtainable with measurement of other quantities at the same or at certain later times. If a system is in thermal equilibrium with a heat bath only its temperature is known. This is less than the information required to define a definite quantum state.

Therefore another approach to the measurement problem is to prepare the system so that it is in a well defined quantum state rather than at a definite temperature. For example, one might drive a system with a stable oscillator and detect changes by observation of amplitude or phase modulation of the output. Quantum mechanics does not give a clear prescription for the optimal way of preparing a system so that greatest sensitivity is achieved, and discovery of this optimal way is an important research goal.

Another issue is the electronics. At frequencies from d.c. to the infra red, stimulated emission devices are the only ones available. At higher energies particle counters may be employed. A counter may be in its ground state, emitting no noise whatsoever, until one phonon or photon appears as a result of some change in a system. No[2] successful counter of this type has ever been developed for the radio region.

We may summarize these comments by stating that systems designed in the traditional way can be improved by going to lower temperatures and employing more nearly perfect crystals. Eventually the energy sensitivity approaches that of a single photon or phonon. In principle even this kind of performance can be exceeded by employment of systems not in thermal equilibrium together with electronics not based on stimulated emission.

Recent Research

By 1974 we had developed, at Maryland, technology involving large elastic solids at room temperature. T was 300 K, Δt was 1 second, τ was 40 seconds and T_N was approximately 5 Kelvin. We could therefore observe changes in elastic solid strain of about 10^{-17} corresponding to energy changes of about 12 degrees.

With AFOSR support we were able to develope a parametric[5] capacitor accelerometer sensor and extend our technology to the liquid helium region. T was 4.2 Kelvin, the fully loaded Q was nearly 1,000,000, and we could observe changes in elastic solid energy of about 0.5 degrees. Thus we improved on our 1974 technology by approximately a factor 25.

The instrumentation depends in an important way on the quality factor Q of the elastic solid. During the past year we studied four materials -- large single crystals of silicon, sapphire, lithium niobate and ruby. These results to be described later illustrate that detailed investigations are required to realize the advantages of going to lower temperatures, for practical instrument designs.

Cooling a solid removes enormous amounts of energy. Sometimes metastable states are "frozen in" and a long period is required for the state of minimum free energy to be reached. Excess noise and poor sensitivity might result from the release of stored energy at a random rate. We observed such effects at liquid nitrogen temperatures, but not at liquid helium temperatures. No noise measurements have ever been made on the very high Q single crystals at liquid helium temperatures - by very high Q we mean exceeding Q values of ten million.

An attempt was made to measure the noise of the large silicon crystal at 4 Kelvin in the following way. The crystal is relatively soft and fragile. It is "dislocation free". For these reasons we did not wish to risk permanent damage by use of epoxy to cement a sensor to the crystal surface. Therefore, a piezoelectric crystal was bonded to an aluminum structure which served as the mount for this crystal. The coupling was adequate to readily excite the silicon crystal by driving the small piezoelectric crystal with a signal generator.

A series of measurements was carried out during the past few months. The quantity which determines the ratio of noise from the elastic solid to electronics wideband noise is βQ. β is the ratio of the elastic solid energy appearing at the output terminals to the internal energy, and Q is the quality factor. For the arrangement of Figure 2, a βQ less than .3 was observed, with all observed noise arising entirely in the electronics.

We have a large sapphire crystal which is extremely rugged, and hard. Epoxy and other bonding materials are readily removed from its surface. Therefore we decided to obtain a much larger βQ by bonding a small lead zirconate titanate crystal to the large sapphire at its center. This was successful in raising the βQ by two orders, to a value 5, with $Q = 10^7$. This value of βQ is quite adequate to carry out an investigation of the noise originating in the sapphire. Continuing problems with our liquifier did not give enough stable operation time to complete these measurements before March 1, 1979.

THE MEASUREMENT OF NOISE IN MONOCRYSTALS AT CRYOGENIC TEMPERATURES: EXPECTED PROBLEMS AND PROPOSED SOLUTIONS

Wm. S. Davis

April 19, 1979

Introduction

It is planned to make noise measurements of monocrystals of sapphire and/or silicon near the thermodynamic temperature of 5 Kelvin. This report describes some of the expected problems of making such noise measurements with high elastic Q materials and low coupling. Solutions to the problems are also discussed.

Table I summarizes the properties of the silicon and sapphire crystals. Each crystal is supported by a fourpoint rigid suspension built by Jean-Paul Richard. These are shown in figures* 1 and 2. Each is coupled to a small piezoelectric ceramic transducer (pzt-4). For the silicon the transducer is expoxied to the mount as shown in figure 1. The transducer for the sapphire is epoxied directly onto the crystal itself.

Figure 3 shows the well known equivalent circuit for one mode of an elastic solid coupled to a transducer and amplifier. Resistors R_1 and R_2 couple Brownian motion energy into the crystal mode. This energy is proportional to the thermal temperature T. Other processes such as non-equilibrium effects and the current noise of the amplifier also put energy into the crystal. The effective noise temperature is defined for the purposes of this report to be the thermal temperature which R_1 and R_2 would have to have to produce the same noise energy in the crystal that all the sources combined produce. It is the goal of the experiment to measure the effective noise temperature for the fundamental mode of the silicon and/or sapphire crystals near 5 Kelvin.

The problems in making the noise measurement include the following. High Q crystals "ring" for a long time. The noise measurement can be disrupted if the amplitude of the ringing greatly exceeds the noise level. The present

---

* Each section of this report has figures numbered independently.

crystal, transducer, and amplifier combination requires a very small bandwidth to see the energy noise of the crystal over the wideband noise of the amplifier. This in turn requires a very stable reference frequency tuned accurately to the crystal resonance. A relatively small bandwidth is also required in one of the intermediate stages of amplification. Before making the noise measurements electronics must be carefully designed, built, and tuned to solve the above foreseeable problems. This is discussed in the following sections.

Summary of Noise Analysis

Consider the electronics of figure 4. x(t) and y(t) are output voltages which are slowly varying functions of time. Let G be the overall gain of the electronics, and let B(ω) be the complex transfer function of the Butterworth low pass filter after its contribution to the overall gain has been factored out.

$$B(\omega) = \frac{1}{1 + i\omega\sqrt{2}\,\tau_f - \omega^2\tau_f^2}$$

$$|B(\omega)|^2 = \frac{1}{1 + \omega^4\tau_f^4}$$

$$B(0) = 1$$

If the input voltage to the preamp is noise only, described by spectral density $e_{in}(\omega)$, then

$$\langle x^2 + y^2 \rangle = G^2 \int_{-\infty}^{+\infty} \frac{1}{2}\left[\left|B(\omega-\omega_r)\right|^2 + \left|B(\omega+\omega_r)\right|^2\right] e_{in}^2(\omega)\, d\omega$$

$$= G^2 \int_{-\infty}^{+\infty} \frac{e_{in}^2(\omega+\omega_r)\, d\omega}{1 + \omega^4\tau_f^4} \qquad (1)$$

where ω_r is the reference frequency of the lock-in amplifier. Further linear filtering of x and y, either analog or digital, will modify the above noise equation. For filtering relevant to this report,

$$\langle \dot{x}^2 + \dot{y}^2 \rangle \tau_f^2 = G^2 \int_{-\infty}^{+\infty} \frac{\omega^2 \tau_f^2}{1 + \omega^4 \tau_f^4} \, e_{in}^2(\omega + \omega_r) \, d\omega \quad (2)$$

$$\langle (x + \dot{x}\tau_o)^2 + (y + \dot{y}\tau_o)^2 \rangle =$$

$$G^2 \int_{-\infty}^{+\infty} \frac{1 + \omega^2 \tau_o^2}{1 + \omega^4 \tau_f^4} \, e_{in}^2(\omega + \omega_r) \, d\omega \quad (3)$$

It can be shown that in the vicinity of the resonance of the crystal (figure 3) the voltage spectral density at the preamp input is given by,

$$e_{in}^2(\omega + \omega_o) = e_f^2(\omega_o) + e_2^2(\omega_o) + \frac{j_f^2(\omega_o)}{\omega_o^2 C_2^2}$$

$$+ \frac{(\beta Q)^2}{1 + \omega^2 \tau_o^2} \left[e_1^2(\omega_o) + e_2^2(\omega_o) + \frac{j_f^2(\omega_o)}{\omega_o^2 C_2^2} \right] \quad (4)$$

The above assumes the following:

$$|\omega| << \omega_0$$

$$\beta Q \frac{1}{\omega_0 C_2 R_2} >> 1$$

$$Q^2 \beta >> 1$$

and that the spectral densities of the noise sources are slowly varying with frequency. Notice that the input spectral density divides naturally into two parts, a wideband part (the first three terms) and a narrowband part (term with $1 + \omega^2 \tau_0^2$ in denominator). The narrowband term is proportional to the spectral density of the energy of the crystal for the mode being observed. The noise energy of the crystal comes from $e_1(\omega)$, $e_2(\omega)$, $j_f(\omega)$, and possibly other sources which are not included in the analysis. If thermal Brownian motion is the only source of noise then

$$e_1^2(\omega_0) + e_2^2(\omega_0) = \frac{2}{\pi} k T (R_1 + R_2)$$

The effective noise temperature (T_n) of the $R_1 + R_2$ combination is defined for this report to be the thermodynamic temperature they would have to have to produce the same narrowband noise as all the noise sources combined. Thus,

$$T_n = \frac{e_1^2(\omega_0) + e_2^2(\omega_0) + \frac{j_f^2(\omega_0)}{\omega_0^2 C_2^2} + \text{other sources}}{\frac{2}{\pi} k (R_1 + R_2)}$$

It should be emphasized that this noise temperature describes only the narrowband part of the noise, those processes contributing to noise energy in the crystal mode itself.

Let $e_w^2(\omega_o)$ be the sum of the three wideband terms,

$$e_w^2(\omega_o) = e_f^2(\omega_o) + e_2^2(\omega_o) + \frac{\dot{j}_f^2(\omega_o)}{\omega_o^2 C_2^2}$$

Then equation 4 for the input spectral density can be rewritten,

$$e_{in}^2(\omega+\omega_o) = e_w^2(\omega_o) + \frac{1}{1+\omega^2\tau_o^2}\,\frac{2\beta Q k T_n}{\pi \omega_o C_2}$$

The results for calculations of the linear filtering given by equations 1, 2, and 3 are shown next. It is assumed that the reference frequency is equal to the crystal frequency, $\omega_r = \omega_o$.

$$\langle x^2 + y^2 \rangle =$$

$$G^2 e_w^2(\omega_o)\frac{\pi}{\sqrt{2}\,\tau_f} + \frac{G^2 2\beta Q k T_n}{\omega_o C_2 \sqrt{2}\,\tau_f}\,\frac{\frac{\tau_f}{\tau_o} + \sqrt{2}}{\frac{\tau_o}{\tau_f} + \frac{\tau_f}{\tau_o} + \sqrt{2}} \qquad (5)$$

$$\langle \dot{x}^2 + \dot{y}^2 \rangle \tau_f^2 =$$

$$G^2 e_w^2(\omega_o)\frac{\pi}{\sqrt{2}\,\tau_f} + \frac{G^2 2\beta Q k T_n}{\omega_o C_2 \sqrt{2}\,\tau_f}\,\frac{\frac{\tau_f}{\tau_o}}{\frac{\tau_o}{\tau_f} + \frac{\tau_f}{\tau_o} + \sqrt{2}} \qquad (6)$$

$$\langle (x + \dot{x}\tau_o)^2 + (y + \dot{y}\tau_o)^2 \rangle =$$

$$G^2 e_w^2(\omega_o)\frac{\pi}{\sqrt{2}\,\tau_f}\left(1 + \frac{\tau_o^2}{\tau_f^2}\right) + \frac{G^2 2\beta Q k T_n}{\omega_o C_2 \sqrt{2}\,\tau_f} \qquad (7)$$

No approximations were made in evaluating the integrals for the above. Note the following relationship,

$$\langle (x + \dot{x}\tau_o)^2 + (y + \dot{y}\tau_o)^2 \rangle =$$

$$\langle x^2 + y^2 \rangle + \langle \dot{x} + \dot{y}^2 \rangle \tau_o^2$$

Table I gives the expected values for the elements of the equivalent circuits of the silicon and sapphire. There is an expected error of $\lesssim$ 20% for the sapphire parameters. Due to the uncertainity of β for silicon only limits exist for several of its parameters. The voltage and current noise of the FET amplifier to be used has not yet been measured at 3468 and 18642 hertz. At 1755 hz the noise was measured as,

$$e_f(\omega) = \frac{1.8 \times 10^{-9} \frac{\text{volts}}{\sqrt{\text{hertz}}}}{\sqrt{2\pi}} = .72 \times 10^{-12} \frac{\text{volts}}{\sqrt{\text{rad/sec}}}$$

$$j_f(\omega) = \frac{4.0 \times 10^{-15} \frac{\text{amps}}{\sqrt{\text{hertz}}}}{\sqrt{2\pi}} = 1.6 \times 10^{-15} \frac{\text{volts}}{\sqrt{\text{rad/sec}}}$$

for BF817 FET

For the parameters in the table the effect of the current noise can be neglected. The expected noise temperature for both crystals is the thermal temperature of 4 to 5 Kelvin. R_2 has not been directly measured yet for either crystal. If the electronic Q of the piezoelectric transducers is estimated conservatively at 50 then the effect of R_2 on the Q of the crystal, the narrowband noise, and the wideband noise can be neglected.* Next the time constant τ_f of the filters

*Mechanical losses in the piezoelectric, the epoxy, and the suspension contribute to R_1.

will be chosen so that the expected wideband and narrowband outputs are equal. Table II lists the values for τ_f and the expected total noise. These numbers are to be used at present for design purposes only. After better measurements of the noise and parameters are made there could be considerable differences.

To obtain the narrowband part of the noise, first the total noise (wideband plus narrowband) will be measured. The wideband part alone can be determined by slightly detuning the reference oscillator of the lock-in amplifier so that the narrowband part falls outside the overall bandwidth. Substracting then yields the average narrowband output. From this measurement and equations 5, 6, or 7 the noise temperature can then be computed.

Crystal Transient Reduction

During a given liquid helium run the crystal will be excited many times above the noise level to obtain a measurement of its frequency and Q. An accurate frequency and Q measurement is needed for noise measurements. However, this transient can interfere with the noise measurements. Waiting for it to die away could take a long time if the Q is high. The amplitude decay time, τ_o, is 8 1/6 hours for the silicon described in Table I. For the sapphire $\tau_o = 990$ seconds. Thus to decay by a factor of 10^6 the silicon requires 4.7 days, while the sapphire needs only 3.8 hours. Therefore, measurements of the silicon noise will be delayed for a substantial amount of time. With the present Q noise measurements of the sapphire will not be substantially delayed by its excitation transient. However, future transducers, capacitive or inductive instead of ceramic piezoelectric, will by design produce much higher Q's for all crystals. This section briefly discusses some ways to reduce the transient itself or its effects on the noise measurement.

The crystal is excited by applying a sinusoid voltage at the crystal frequency across C_2 (figure 3) for a short interval of time. The transient can then be reduced by applying another sinusoid of appropriate phase and duration. This technique has been tried successfully with the silicon bar at liquid helium temperatures. However, it does not enable one to closely approach the noise energy of the crystal due to the relatively large amounts of wideband noise compared to the low level of noise energy expected in the crystal. Reducing the bandwidth does decrease the wideband noise, but also increases the response time of the filters. This means waiting a long time to get information about the phase and amplitude of the transient. For the silicon described by Table I as the transient approaches the level of the noise

energy in the crystal, the time constants of the filters needed to resolve it exceed the damping time of the antenna. Thus this method will not eliminate the lowest levels of the transient.

A second method for reducing the transient is to increase the damping by adding an external resistor across C_2. However, unless C_2 can be made effectively smaller (increased coupling), significant energy from the crystal cannot be dissipated by the resistor. This can be done by adding an appropriate inductor across C_2 also. In order to reduce the transient to the level of the energy noise, the resistor and probably also the inductor will have to be cooled to the same temperature as the crystal. Katsunobu Oide and others at the University of Tokyo have used feedback to reduce the noise temperature of a resistor.[1] This technique might be applicable to removing the transient from high Q, low coupling crystals, but the detailed analysis has yet to be done by this author. After the transient is gone the external resistor and inductor must be removed to make the noise measurement.

Electronic filtering, either digital or analog can reduce the interference caused by the transient energy in the crystal when noise measurements are made. The x and y outputs of the excited crystal have the following form:

$$x(t) = x_n(t) + x_e\, e^{-t/\tau_0}$$

$$y(t) = y_n(t) + y_e\, e^{-t/\tau_0}$$

The subscript "n" refers to the noise discussed in the previous section, and the subscript "e" refers to the excitation of the crystal above equilibrium at some initial time. The ensemble average outputs are then given by,

$$\langle x^2(t) + y^2(t) \rangle = \langle x_n^2 + y_n^2 \rangle + (x_e^2 + y_e^2)\, e^{-2t/\tau_0}$$

$$\langle \dot{x}^2(t) + \dot{y}^2(t) \rangle \tau_f^2 = \langle \dot{x}_n^2 + \dot{y}_n^2 \rangle + \left(x_e^2 + y_e^2\right) \frac{\tau_f^2}{\tau_o^2} e^{-2t/\tau_o}$$

$$\langle (x(t) + \dot{x}(t)\tau_o) + (y(t) + \dot{y}(t)\tau_o)^2 \rangle =$$

$$\langle (x_n + \dot{x}_n \tau_o)^2 + (y_n + \dot{y}_n \tau_o)^2 \rangle$$

Note that the third linear filter totally removes the excitation transient of the crystal before squaring. In practice the crystal decay time, τ_o, will not be known well enough to remove all the transient. Suppose τ_o' is the value which is used for τ_o. Then the following term must be added to the latter equation above,

$$\left(x_e^2 + y_e^2\right)\left(1 - \frac{\tau_o'}{\tau_o}\right)^2 e^{-2t/\tau_o}$$

For the present silicon and transducer one or more of the above methods can be used to remove the transient if an attempt at measuring the energy noise is made. Increased coupling will improve the effectiveness of these techniques.

Reference Frequency

The lock in amplifier requires a reference oscillator. The results of the noise calculations — equations 5, 6, and 7 — are valid only for the reference frequency sufficiently close to the crystal resonance. When the filter time constant is roughly equal to the decay time of the crystal, it turns out that for all three of the linear filters considered the following condition must be maintained, $\left| \frac{\omega_o - \omega_r}{\omega_o} \right| \ll \frac{1}{Q}$

The crystal frequency must be measured to <u>better than</u> this accuracy. The reference must be tuned to and maintained at this frequency to <u>better than</u> this accuracy throughout the duration of the measurement. Data must be collected for a time greater than the decay time of the crystal. Thus the stability and accuracy requirements for each of the crystals is,

silicon, accuracy and stability of better than one part in 3×10^8 over a time greater than 8 hours.

sapphire, accuracy and stability of better than one part in 6×10^7 over a time greater than ¼ hour.

Devices are commercially available which have the needed stability and accuracy. They cost several thousands of dollars to buy and several hundred of dollars per month to rent. These alternatives might be considered.

Frequency measuring and generating devices of sufficient accuracy and stability have been constructed from equipment which we already have in our possession. The Hewlett Packard 10544A 10 Mhz quartz crystal oscillator has a rated stability of better than one part in 2×10^9 per day. The oscillator and the HP 5216A electronic counter have the needed precision to measure the

crystal frequencies. The 10 Mhz oscillator is also used to generate the reference frequency. This eliminates the need for calibration. Figure 5 shows the phase lock loop which has been used. Note that the 10 Mhz oscillator is not in the loop. A second crystal oscillator is servoed by a voltage which is proportional to the difference between the desired and the generated periods. Prototypes of this frequency synthesizer have been successfully tested for both silicon and sapphire frequencies.

The frequency of the crystal is a function of temperature. McGuigan and others have determined that at liquid helium temperatures the temperature dependence of the resonance frequency of silicon has the following form,[2]

$$\frac{f(T) - f(0)}{f(0)} = 1.82 \times 10^{-10} T^3$$

During a typical run with the cryostat to be used to make our noise measurements the temperature of the experiment changed from 4.4 Kelvin to 5.7 Kelvin over the six day holding period of the dewar. The best temperature stability was about .1 Kelvin per day for the first four days. An adequate noise measurement requires collecting data for a time equal to many decay times. Ten decay times for the silicon is 3.4 days. During this time the frequency of the silicon will drift by about one part in 3×10^8. Thus the best temperature stability is just at the edge of what is needed. Improvements have recently been made in the cryostat which are expected to increase the thermal stability, ie. better heat sinking of the wires going to the experiment. However, this has not yet been tested. Active temperature control can be provided if necessary. Alternatively if the temperature dependence of the frequency is known accurately enough, the reference frequency can be compensated to follow the crystal frequency.

The temperature dependence of the resonance frequency of sapphire has not yet been obtained by this author. Such data has probably been obtained by V. Braginsky. We hope to obtain it in the near future from him or our own measurements. However, the frequency stability requirements for the sapphire presently being tested are less stringent than for silicon by a factor of over 100. Thus noise measurements for the sapphire probably won't need improved temperature stability or compensation.

Gain and Bandwidth

Careful choice of gain and bandwidth of the stages of the electronics of figure 4 is needed to obtain an adequate output without saturation. Consider first a specific example, $x^2 + y^2$ for the sapphire. For a .7 volt rms output for each of x and y a total gain of 10^{10} is needed. The gain in the low pass filters should be no more than 100 due to dc drifts. Thus the gain of the preceeding stages should be greater than 10^8. The detectors of the lock in amplifier (a PAR 129) begin to saturate at about one volt rms of noise. The narrowband signal will not cause these detectors to saturate but the wideband noise might. The effective noise bandwidth of the preamp and postamp which will not produce this saturation is given by

$$10^8 \times 2 \frac{nv}{\sqrt{hz}} \times \sqrt{\Delta f} < 1 \text{ volt}$$

assuming 2 $nv/\sqrt{hz}$ wideband noise at the preamp input. Thus we need $\Delta f < 25$ hertz. This narrow bandwidth at 18642 hertz might just barely be attainable by the four cascaded LC tuned amplifiers of the postamp. This device presently has a bandwidth of about 78 hertz. More careful tuning and slight amounts of positive feedback might bring the bandwidth down some more.

Table III gives the expected upper limit for the postamp bandwidth for silicon and sapphire and each of the three linear filters. With the possible exception of sapphire at 25 hz = Δf, amplifiers with quartz crystal filters or a combination of down conversion and crystal filters will probably be needed to achieve these narrow bandwidths.

Conclusion

The noise measurement for the sapphire appears feasible with a moderate effort put into further electronic development. The major work which remains to be done is the development of a postamp with narrow enough bandwidth. It is well within technical feasibility.

The noise measurement for the silicon is more difficult, due mainly to the low coupling. Much more development is needed than for the sapphire. It might be more feasible to improve the coupling instead. This would relax the present requirements for transient removal, frequency and temperature stability, and bandwidth by giving a larger energy noise signal and permitting a smaller filter time constant to be used.

Larger couplings can be achieved with piezoelectric transducers and epoxy, but this reduces the Q. As a consequence the Brownian motion noise of the crystal comes more from loss processes in the transducer than from the crystal (and its suspension). The sapphire presently being used had a Q of 4×10^8 at 4 Kelvin before the piezoelectric was attached. The present Q of 58×10^6 means that at equilibrium roughly 15% of the energy noise to be observed comes from the crystal (and its suspension). Possible future experiments with these crystals could have β's as large as 10^{-7} with inductive and capacitive transducers while maintaining high Q. These would, however, require separations of about .1 mm between the transducer and the end of the crystal. The use of a properly matched SQUID amplifier instead of an FET would also be a significant improvement.

REFERENCES

1) Katsunobu Oide, Yujiro Ogawa, and Hiromasa Hirakawa, "Artificial Cold Resistors," Japanese Journal of Applied Physics, 17,429 (1978).

2) D.F. McGuigan, C.C. Lam, R.Q. Gram, A.W. Hoffman, D.H. Douglass, and H.W. Gutche, "Measurements of the Mechanical Q of Single-Crystal Silicon at Low Temperatures," Journal of Low Temperature Physics, 30, 621 (1978).

TABLE I

PROPERTIES OF MONOCRYSTALS COUPLED TO TRANSDUCERS

material	mass (kg)	length (cm)	fundamental mode frequency at 5 Kelvin (hz)	loaded Q at 5 Kelvin	β at 5 Kelvin
Silicon	15½	135	3467.8	320×10^6	$\lesssim 10^{-9}$
Sapphire	5.2	25	18,642	58×10^6	$\gtrsim 10^{-7}$

	τ_o (sec)	L_1 (henries)	$R_1 + R_2$ (ohms)	C_1 (farads)	C_2 (farads)	$\frac{\beta kT}{C_2}$ (volts)^2
Silicon	29,400	$\gtrsim 3 \times 10^9$	$\gtrsim 2 \times 10^5$	$\lesssim 7 \times 10^{-19}$	7.0×10^{-10}	$\lesssim (10^{-11})^2$
Sapphire	990	8.1×10^3	1600	9.0×10^{-17}	9.0×10^{-10}	$(88 \times 10^{-12})^2$

TABLE II

Expected Values of τ_f and Noise when Wideband Noise Equals Narrowband Noise

		$x^2 + y^2$	$(\dot{x}^2 + \dot{y}^2)\ \tau_f^2$	$(x + \dot{x}\tau_o)^2 + (y + \dot{y}_o)$
Silicon	τ_f (sec)	28,000	111,000	44,300
	total noise referred to preamp input (volts)	10^{-11}	5×10^{-12}	8×10^{-12}
Sapphire	τ_f (sec)	216	890	590
	total noise referred to preamp input (volts)	10^{-10}	6×10^{-11}	7×10^{-11}

TABLE III

Expected Upper Limit of Postamp Bandwidth to Prevent Saturation of Lock-in Amplifier

	$x^2 + y^2$	$(\dot{x}^2 + \dot{y}^2)\ \tau_f^2$	$(x + \dot{x}\tau_o)^2 + (y + \dot{y}\tau_o)^2$
Silicon Δf (hertz)	.25	.063	.16
Sapphire Δf (hertz)	25	9	12

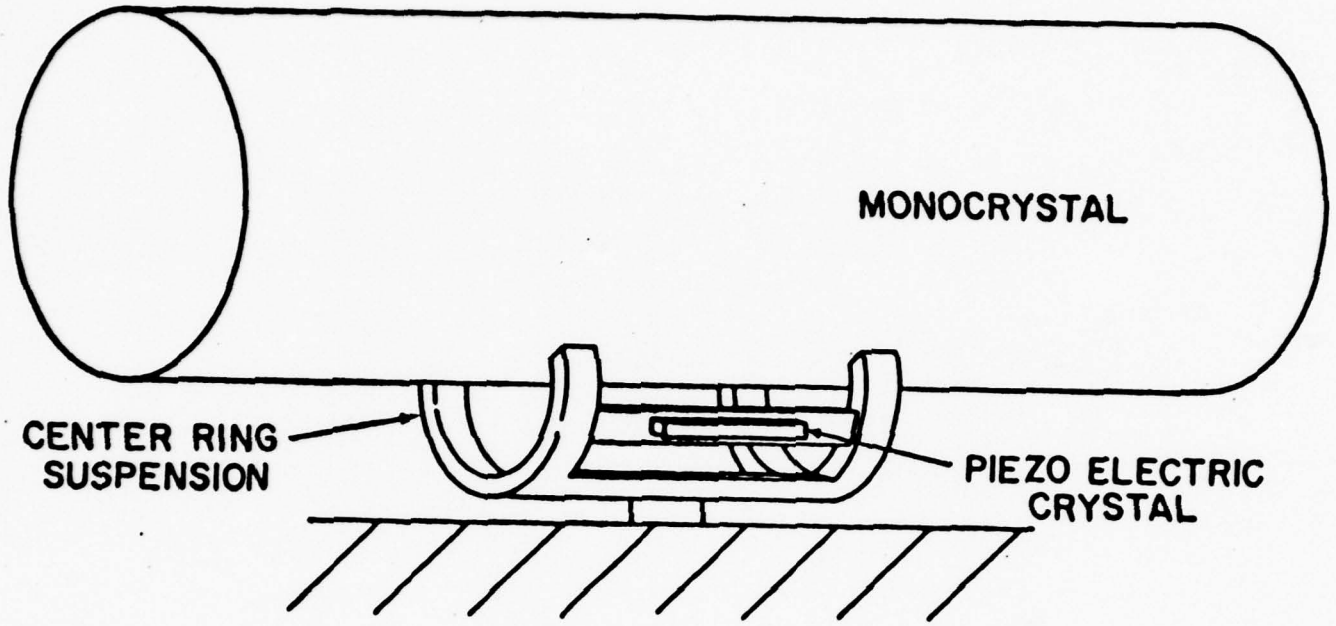

Figure 1

Silicon Suspension

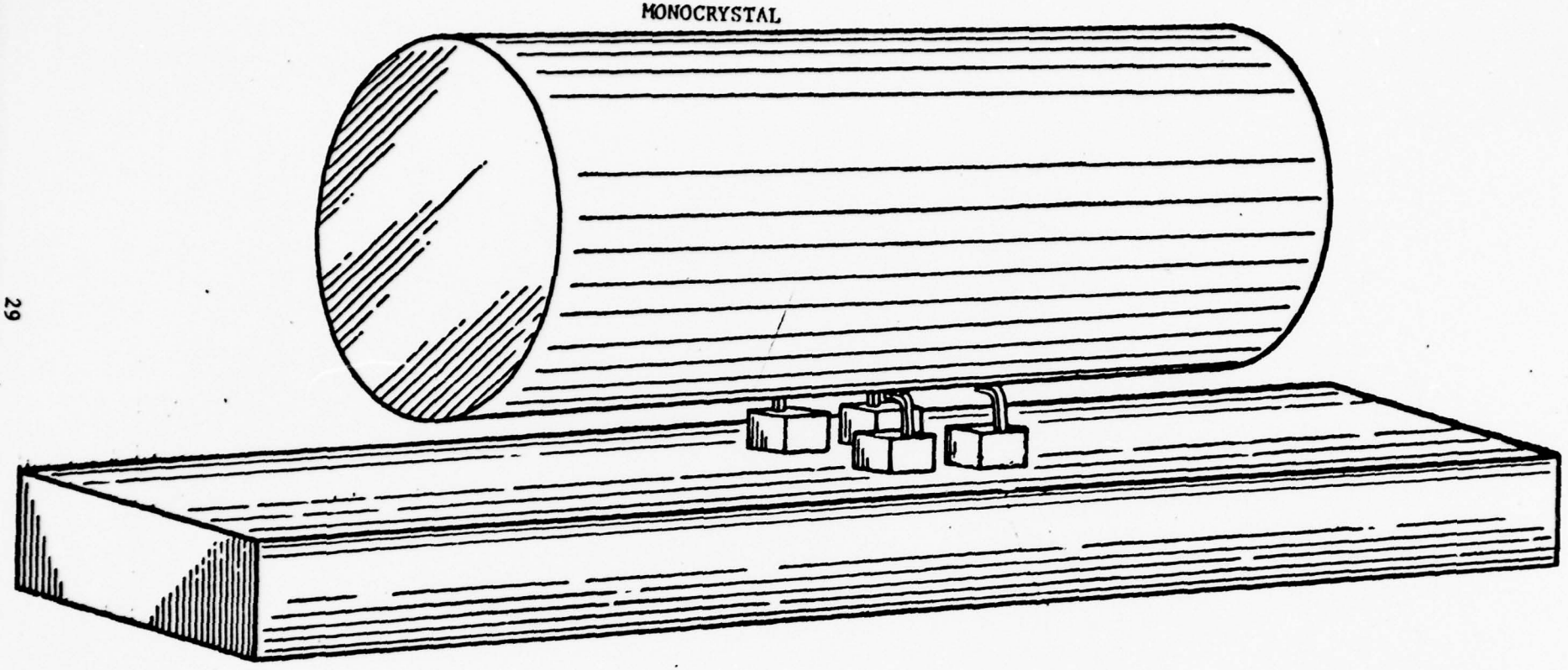

Figure 2
Sapphire Suspension

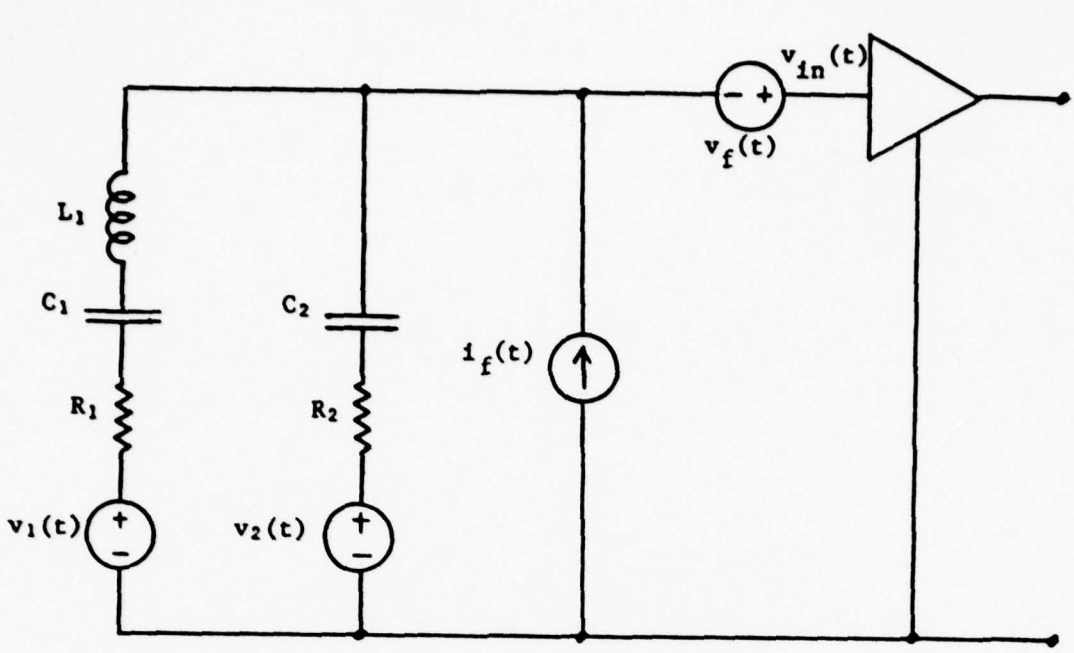

$$\omega_0^2 = \frac{1}{L_1}\left(\frac{1}{C_1} + \frac{1}{C_2}\right) \qquad \text{resonant frequency}$$

$$\beta = \frac{C_1}{C_1 + C_2} \qquad \text{coupling}$$

$$\tau_0 = \frac{2L_1}{R_1 + R_2} \qquad \text{amplitude decay time}$$

$$Q = \frac{\omega_0 L_1}{R_1 + R_2} \qquad \text{quality factor}$$

$$1 = L_1 C_2 \omega_0^2 \beta$$

	Time Domain	Spectral Density
crystal noise	$v_1(t)$	$e_1(\omega)$
transducer noise	$v_2(t)$	$e_2(\omega)$
amplifier noise	$v_f(t)$	$e_f(\omega)$
	$i_f(t)$	$j_f(\omega)$

$$\langle v^2 \rangle = \int_0^\infty e^2(\omega)\, d\omega \qquad \langle i^2 \rangle = \int_0^\infty j^2(\omega)\, d\omega$$

Figure 3, Equivalent Circuit and Definitions

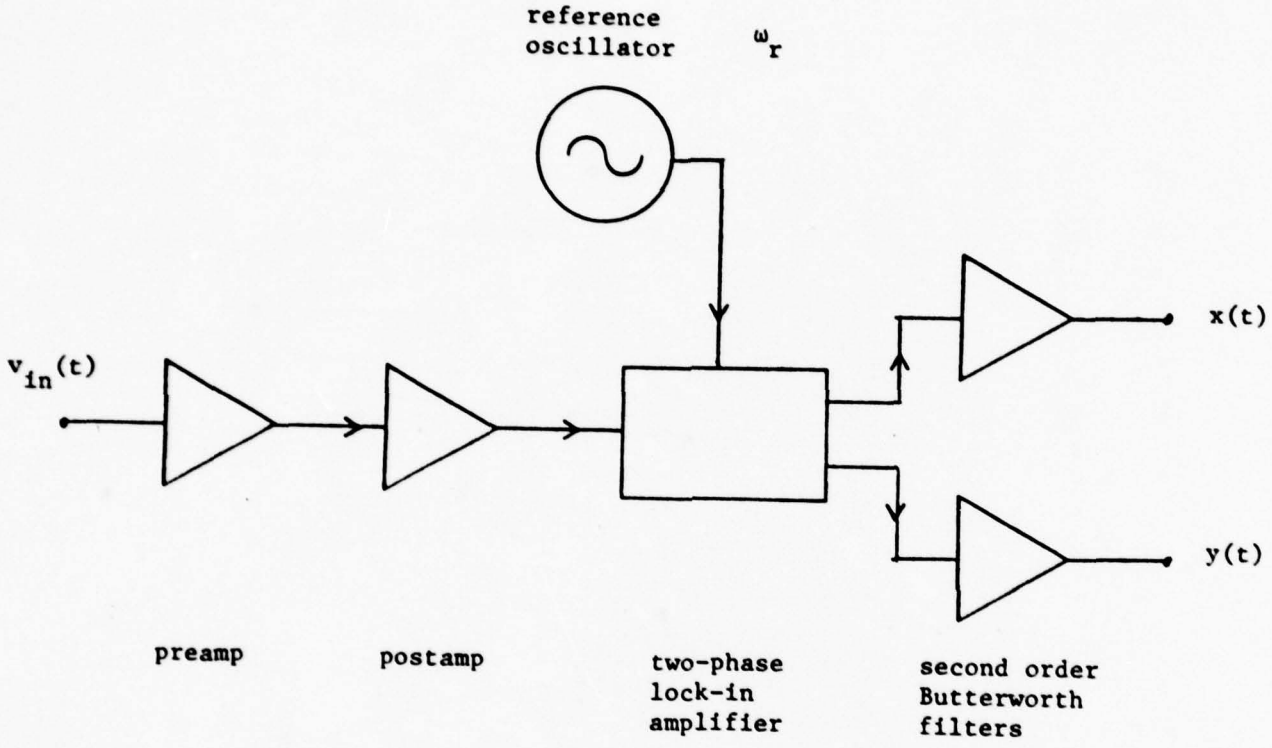

Figure 4, Electronics

x and y may be recorded directly on magnetic tape or undergo further analog processing before being recorded.

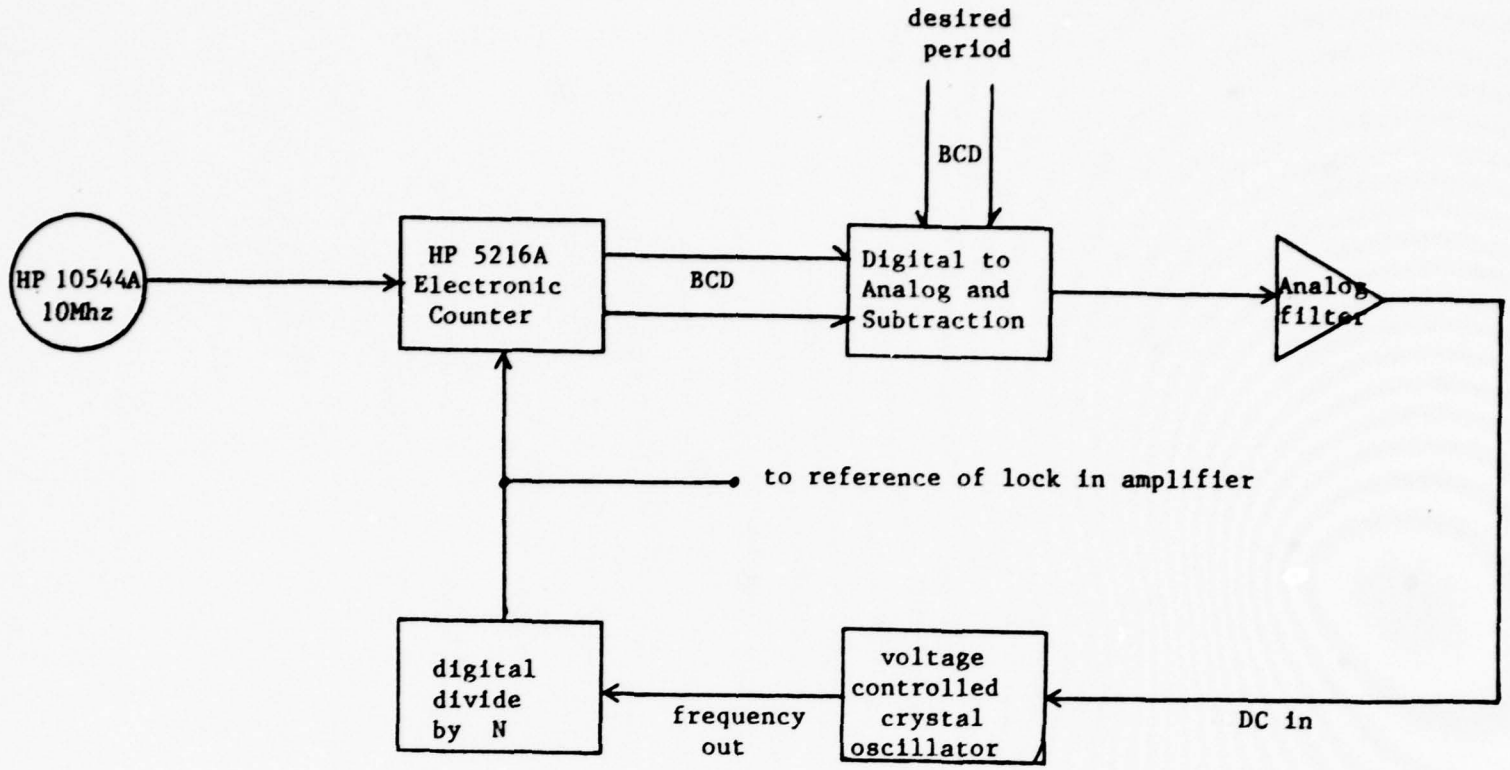

Figure 5, Phase lock loop for generating reference for noise measurements of crystals

Q MEASUREMENTS AT CRYOGENIC TEMPERATURES

As noted in equation (5), the ultimate sensitivity which can be attained in measurements of changes in energy of any elastic solid detection depends on the free oscillation Q--decay time τ. A program to study the low temperature noise must begin with Q measurements. The details of the mount, and instrumentation will depend critically on the Q values.

During the past year detailed measurements of the Q of the fundamental longitudinal mode of ruby, sapphire, lithium niobate and silicon were carried out. All crystals were cylindrical rods. Most of the measurements were made supporting the crystals by aluminum four point suspensions. One measurement (ruby) was made with a tungsten wire suspension as shown in Figure 1. Either end capacitor plate or piezoelectric ceramic crystals were employed.

Ruby is sapphire doped with (paramagnetic) chromium ions. It is being studied in order to assess the importance of paramagnetic ions in affecting the Q. Most materials contain a certain amount of paramagnetic ions as impurities. At sufficiently low temperatures the specific heat of the lattice vibrations of a crystal will be extremely small -- so small that measurements would be affected by the heating effect of the high energy cosmic rays. Control of the specific heat by doping with paramagnetic impurities may be a very useful technique.

The instrumentation of a nearly perfect crystal to observe its low temperature properties is enormously simplified if the crystal is piezoelectric. It is therefore of interest to explore single crystal materials such as lithium niobate.

MONOCRYSTAL MATERIAL	MASS (kg)	TEMPERATURE (Kelvin)	FREQUENCY (Hertz)	SUSPENSION	TRANSDUCER	Q (10^6)
Ruby	.96	4.2	15,028	Tungsten wire, figure 1	Piezoelectric ceramic glued to crystal	20
Ruby	1.44	4.3	26,743	Aluminum 4 point mount, figure 2	End face capacitor	47
Sapphire	5.2	4.3	18,644	Aluminum 4 point mount, figure 2	End face capacitor	400
Silicon	.78	4.3	11,337 (bending mode)	Aluminum 4 point mount, figure 2	Piezoelectric ceramic glued to suspension	76
Silicon	15	5.8	3467.8	Aluminum 4 point mount, figure 4	Piezoelectric ceramic glued to suspension	320

RUBY

Two different ruby crystals have been tested. Each is a single crystal of pink sapphire, sapphire doped with .05% chromium. They both have a rough polish on the sides and ends. Their mass and dimensions are;

.96 kg mass, 3.0 cm diameter, 33.1 cm length

1.44 kg mass, 5.0 cm diameter, 18.5 cm length

The .96 kg ruby was suspended with a tungsten wire as shown in figure 1. A pzt-4 piezoelectric ceramic was bonded to the surface of the crystal with Stycast 2850 FT. The Q of the fundamental longitudinal mode at 4.2 Kelvin was 20×10^6. Figure 5 shows Q measurements between 30 and 300 Kelvin.

The 1.44 kg ruby was supported with the four point aluminum suspension shown in figure 2. The end surfaces were coated with aluminum, so that a split capacitor plate could be used to measure the motion. This is shown in figure 3. The Q of the fundamental longitudinal mode at 4.3 Kelvin was 47×10^6.

Results reported in the next sections suggest that the present aluminum four point suspension reduces the Q more than a wire suspension. If this is true then the lower Q of the wire supported ruby would then be due to the piezoelectric transducer.

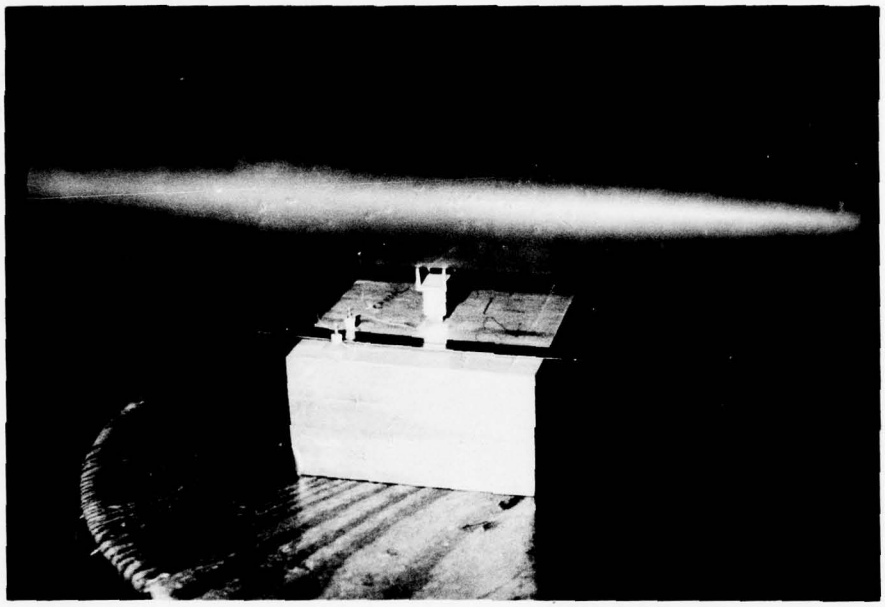

RUBY CRYSTAL

SAPPHIRE

The sapphire crystal was obtained from Union Carbide. It is 25 cm long and 8.25 cm in diameter and has a mass of 5.2 kg. The side surface was unpolished and untreated in any way. The end faces had a rough polish and were coated with aluminum. The four point suspension and capacitor transducer were the same as that used for the 1.44 kg ruby, figures 2 and 3. The Q of the fundamental longitudinal mode at 4.3 Kelvin was about 400×10^6. Douglass has reported measurements of the Q of the quadrapole mode of a 5.6 kg sapphire disk at 4.3 K.[1] The crystal was supported by two ball bearings, centered top and bottom. The result was also $Q = 400 \times 10^6$. Braginsky has also published measurements of the Q of a sapphire crystal.[2] This crystal was a cylindrical rod supported at its center with the wire suspension of figure 1. The result for the longitudinal mode at 4.3 Kelvin was 5×10^9. The wire suspension produced a Q which was an order of magnitude higher than the two rigid suspensions. Factors such as crystal purity and the transducer as well as suspension could have lowered the Q. If, however, mechanical losses were limited by the rigid suspension, then the use of higher Q materials, such as sapphire itself, might reduce these losses. The aluminum alloy which has been used at Maryland for all rigid suspensions is alloy 6061. This alloy has a mechanical Q of about 10^6 at liquid helium temperatures. Hirakawa has discovered that aluminum alloy 5056 has a Q of 70×10^6 below 20 Kelvin.[3] Our future research into suspensions for sapphire crystals will include four point suspensions made of high Q materials such as aluminum 5056 and sapphire.

The Q's of the 5.2 kg sapphire and the 1.44 kg ruby were measured with the same transducer and suspension. The result for ruby was 8½ times lower. This suggests significant attenuation due the chromium ions in the ruby material.

SILICON

Two different silicon crystals were tested. The smaller of the two was furnished by Texas Instruments. Its mass is .78 kg, diameter 5 cm, and length 17 cm. The sides were etched and the ends unpolished. The Q of the bending mode at 11337 hertz was observed by mounting a pzt-4 piezoelectric transducer under one of the four aluminum suspension points shown in figure 2. The Q as a function of temperature is shown in fiugre 6. At 4.3 Kelvin the Q was 76×10^6.

Data for the 15 kg silicon crystal furnished by Monsanto are given on the next page. The surface of the crystal has not yet been improved. The ends and the sides have visible irregularities resulting from the crystallization process. The crystal was supported by the aluminum four point suspension shown in figure 4. A pzt-4 piezoelectric ceramic was epoxied onto the suspension as shown in this figure. Figure 7 shows the results of Q measurements as a function of temperature. At 5.8 Kelvin the Q was 320×10^6.

Both the above silicon crystals gave a significant drop in Q in the 10 to 15 Kelvin range. The 15 kg silicon shows a minimum at 12 Kelvin. A minimum in the Q of silicon (at 13 Kelvin) has also been observed by McGuiga et al of the University of Rochester.[4] Their 4.9 kg silicon crystal was polished and coated with aluminum on the ends. A split capacitor plate was used at the transducer. The sides were not altered. The crystal was suspended with a tungsten wire and Q measurements were made from 1.3 to 300 Kelvin. The minimum in the Q curve for two different silicon crystals, with different suspensions, transducers, and end face conditions strongly indicates that the mechanism causing the friction comes from a bulk property

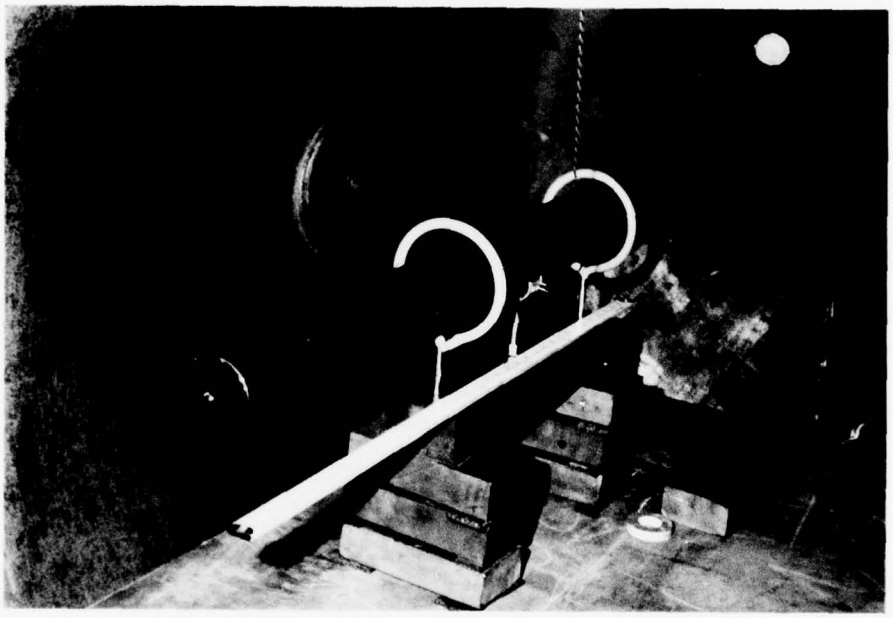

SILICON CRYSTAL

15 kg SILICON CRYSTAL

Crystal Data #99-0491

Weight:	15,465 grams
Diameter:	78.4 mm
Material:	Single Crystal Silicon
Length:	53.5 inch
Conductivity Type:	P-type
Resistivity:	~ 20 ohm cm (seed end) ~ 14 ohm cm (opposite end)
Major Impurities:	Oxygen: ~ 10^{18} atoms/cc
	Carbon: ~ 10^{17} atoms/cc
	Boron: ~ 8×10^{14} atoms/cc
Method of Growth:	Czochralski (pulled from melt contained in quartz crucible)
Rate of Crystallization:	100 mm/hr.

This very large crystal is described as "dislocation free". Industry employs such a description for crystals having less than 10 dislocations per square centimeter.

of the silicon. Observations of the silicon bending mode data, although they don't show a minimum due to insufficient data, also support this conclusion. Both the Rochester 4.9 kg and Maryland 15 kg crystals were supplied by Monsanto. Both are p-type boron doped with a similar level of other impurities. The Rochester group suggests that it is the boron impurity which produces the Q minimum. It would be most interesting to make similar measurements for a n-type silicon crystal.

At 5.8 Kelvin the Maryland 15 kg silicon crystal had a Q of 320×10^6. At the same temperature the Rochester group reports a Q over three times higher. This difference is probably due to losses from the suspension and/or piezoelectric transducer. Four point suspensions of higher Q will be tried in future experiments. Possible materials include aluminum 5056, silicon, and quartz. The latter two materials offer the possibility of an increased number of chemical bonds between the surfaces of the crystal and the suspension, and presumably lower losses at these points. The sides and ends of the 15 kg crystal will be ground and polished, and a capacitor transducer installed.

There is one point in the Q curve for the 15 kg silicon which is significantly lower than then the others near the same temperature (16 Kelvin of figure 7). It is possible that this Q was measured with an amplitude much greater than the other measurements. Alternatively it may have a bad measurement. The data is now being carefully studied.

CONCLUSION

Many Q measurements of monocrystals of ruby, sapphire, and silicon at cryogenic temperatures are presented. Comparison of these results with that of other groups suggests that higher Q's can be achieved with rigid suspensions of higher Q material.

The minimum in the Q curve of silicon between 10 and 15 Kelvin first observed by the group at the University of Rochester has been duplicated in a crystal of similar composition but different suspension, transducer, and end surfaces. This strongly supports the Rochester group's suggestion that mechanical losses in silicon at these temperatures are due to internal bulk properties of the material.

REFERENCES

[1] D. E. Douglass, "Gravitational Wave Experiments", International Meeting on Experimental Gravitation (Pavia, September 17-20, 1976), p. 331.

[2] V. B. Braginsky, "The Conditions for the Detection of High Frequency Gravitational Wave Burst of Nonterrestrial Origin", International Meeting on Experimental Gravitation (Pavia, September 17-20, 1976), p. 224.

[3] H. Hirakawa, private communication.

[4] D. F. McGuigan, C. C. Lam, R. Q. Gram, A. W. Hoffman, and D. H. Douglass, "Measurements of the Mechanical Q of Single-Crystal Silicon at Low Temperatures", Journal of Low Temperature Physics, 30, 621 (1977).

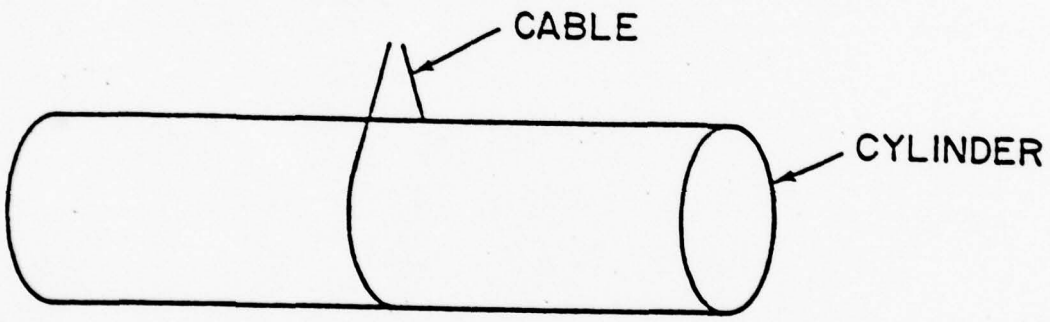

Figure 1. Tungsten wire suspension for .96 kg ruby crystal.

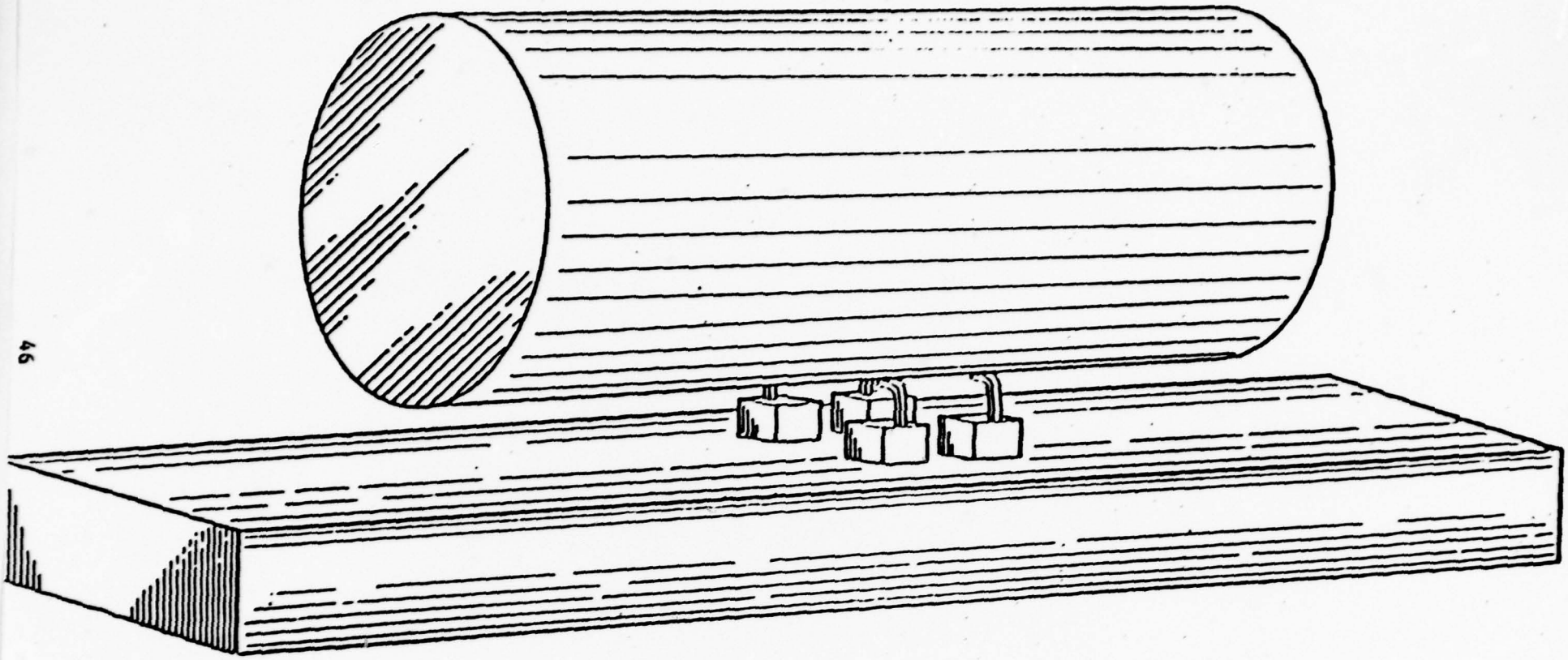

Figure 2. Aluminum four point suspension for 1.44 kg ruby, 5.2 kg sapphire, and .78 kg silicon crystals.

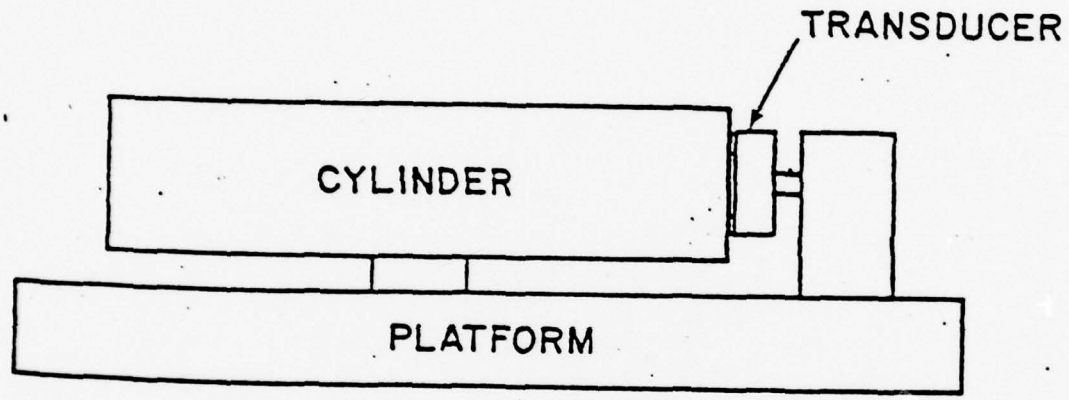

Figure 3. Capacitor transducer.

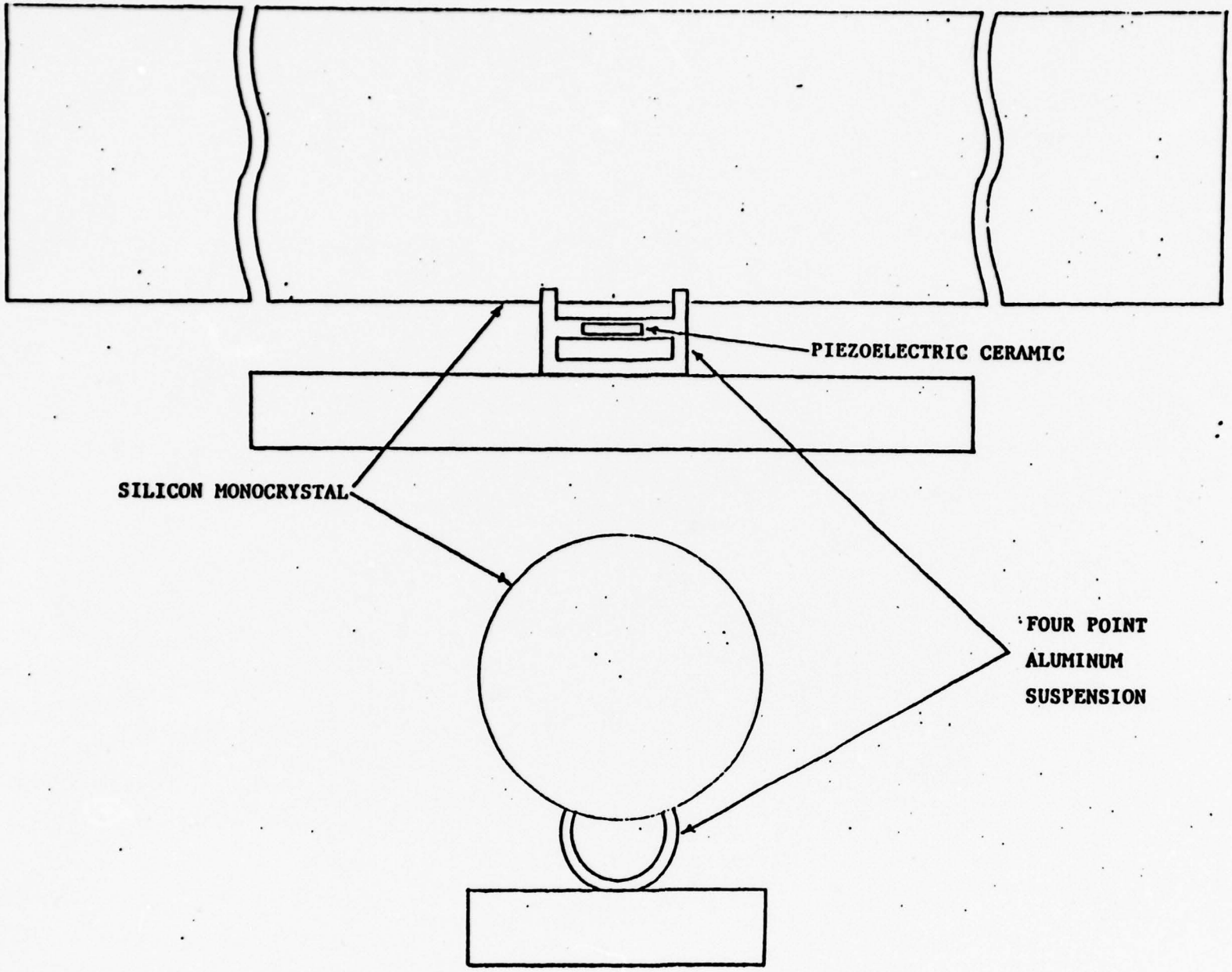

Figure 4. Aluminum four point suspension for 15 kg silicon crystal.

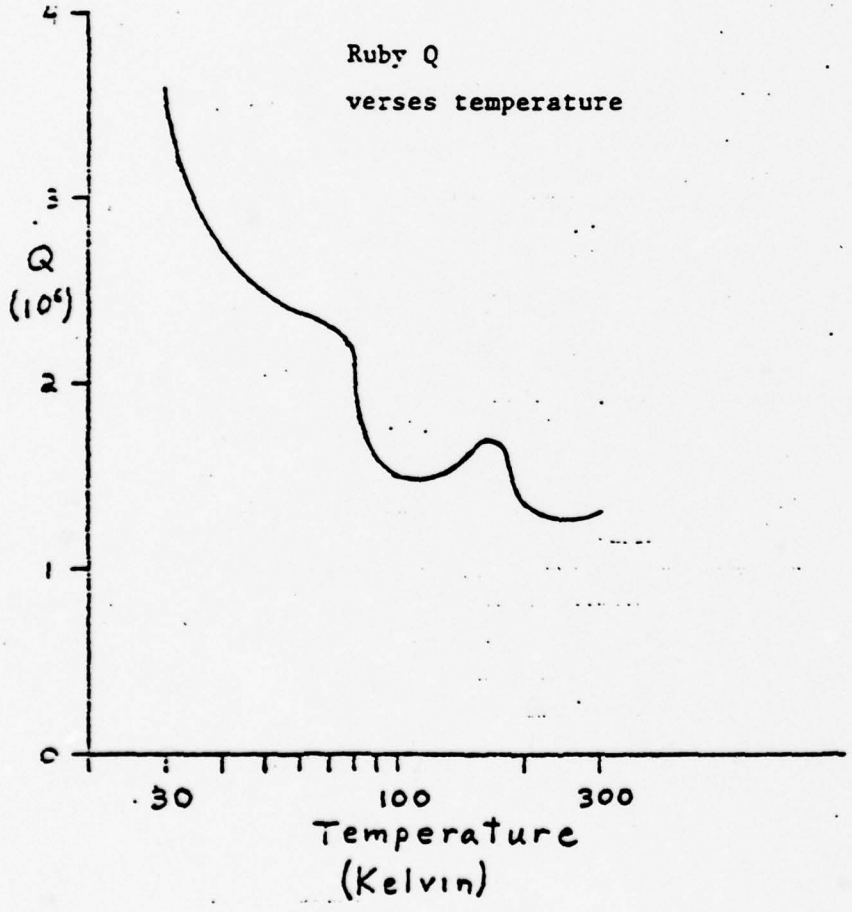

Figure 5. Q of longitudinal mode of .96 kg ruby crystal.

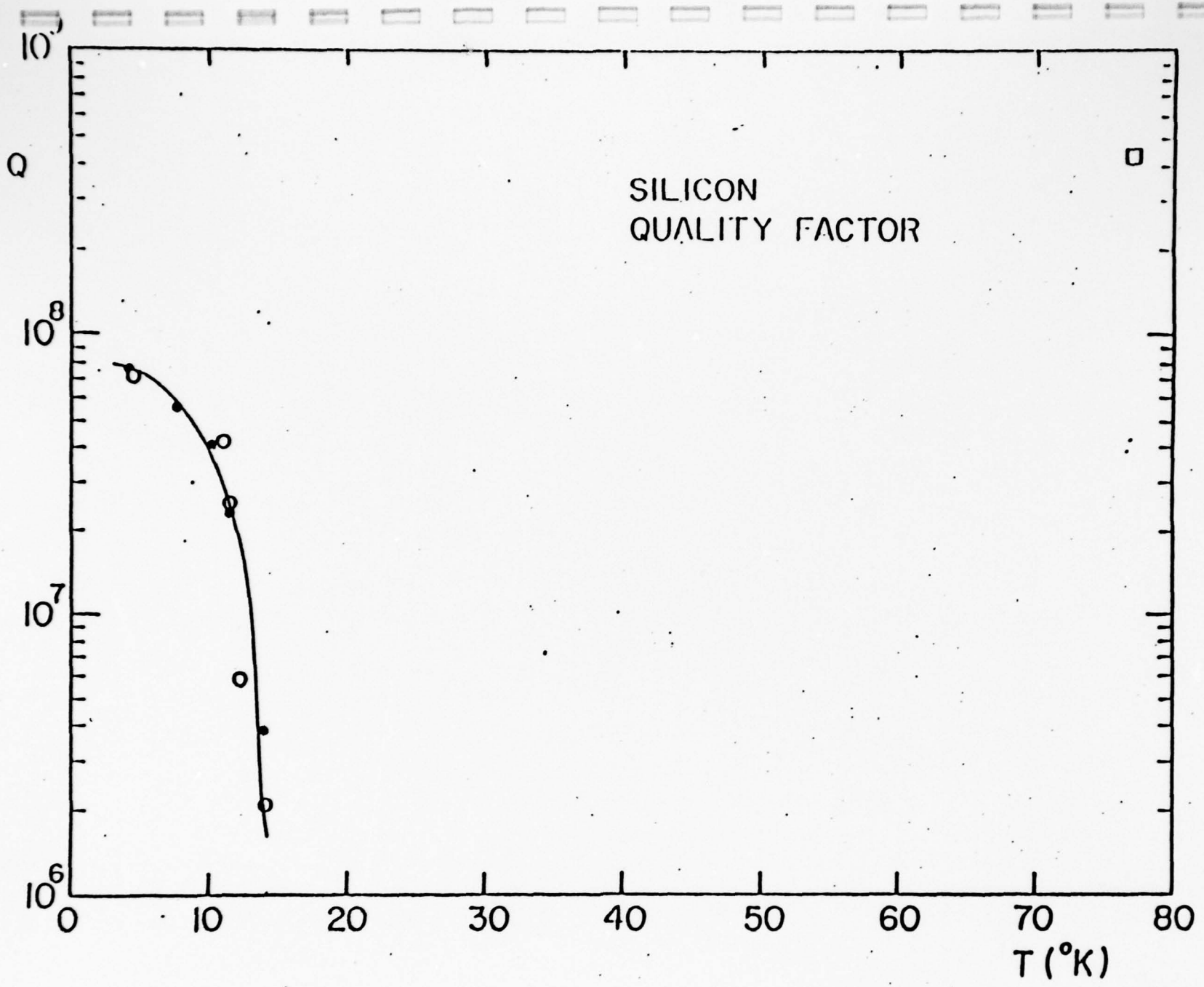

Figure 6. Q of bending mode of .78 kg silicon crystal.

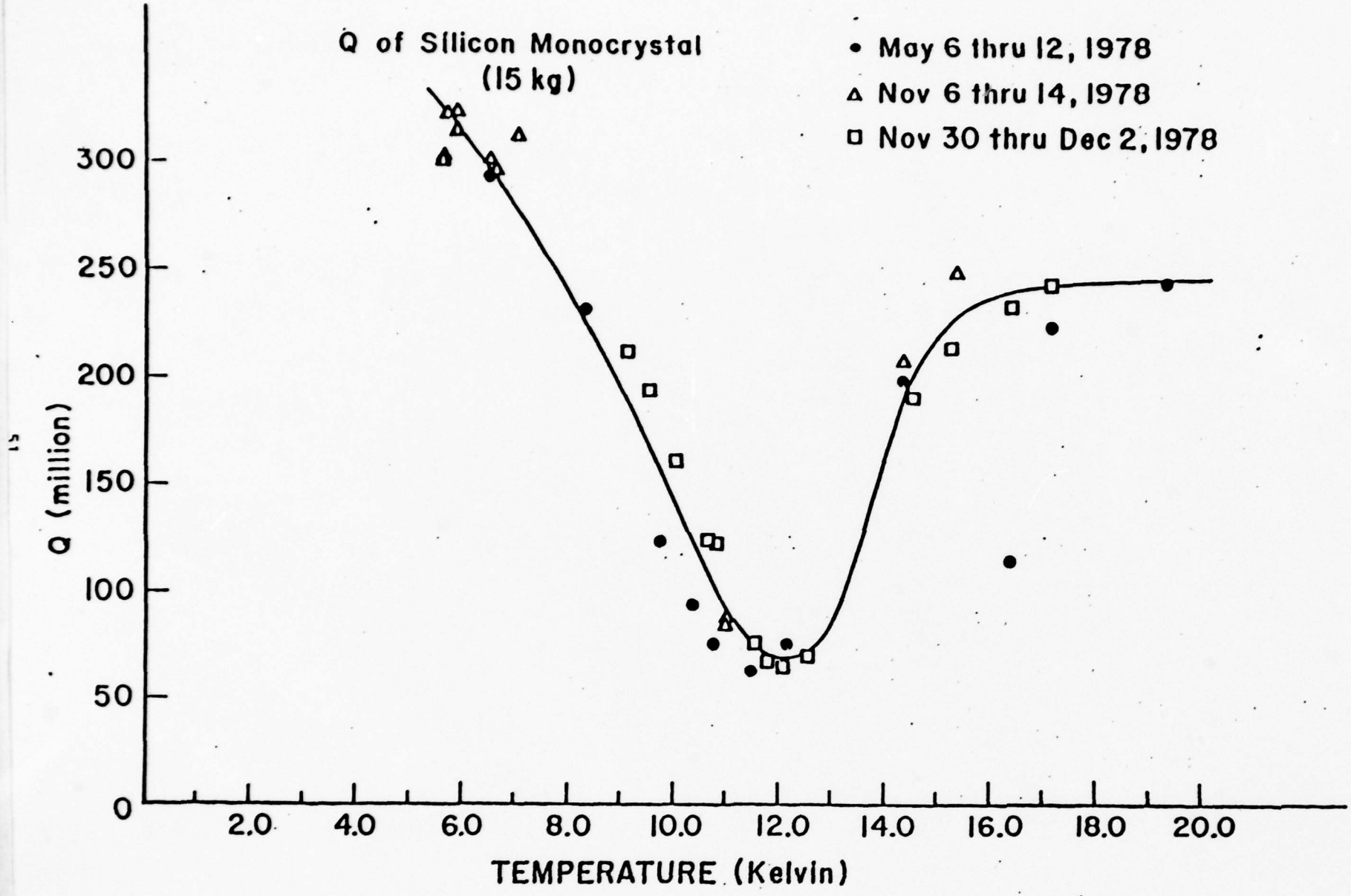

Figure 7. Q of longitudinal mode of 15 kg silicon crystal.

LITHIUM NIOBATE AT CRYOGENIC TEMPERATURES

The planar piezoelectric coupling constant of a small lithium niobate disc was measured at 300 K, 77 K, and 4.2 K. The result was about 10^{-3} for all three temperatures. This agrees with a theoretical calculation using the piezoelectric and elastic constants of lithium niobate. The frequency was about 200 khz. The overall Q was also measured at 4.2 K and found to be 25,000 to 30,000.

The lithium niobate ($LiNbO_3$) crystal was obtained from Crystal Technology Inc. It was a disc with diameter .79 inches and thickness .05 inches. Silver was vacuum deposited on each side. A small area of the silver, about two square millimeters, was removed from the center of each side of the disc. Two AWG 26 tinned copper wires were attached with conducting epoxy TRA-CON BB-2902. The epoxy made a bond with the crystal and with the silver. Figure 1 shows how the crystal was mounted in a small vacuum chamber. The chamber was immersed in liquid nitrogen or liquid helium in a small glass dewar.

Figure 2 shows the circuit used to measure the electromechanical coupling of the crystal. The capacitance of the coaxial line from A to B was measured with the crystal and the capacitance box disconnected.

Figure 3 shows the equivalent circuit. Only two sources of loss are shown in the circuit. There are certainly others. The cables going from the oscillator to "signal in" and from "signal out" to the oscilloscope each have a capacitance of about 100 pf. Hence, from point A the "signal in" and "signal out" are essentially grounded. Let Z be the impedance of point A to ground. The amplitude of the signal observed on the oscilloscope will be proportional to $|Z|^{-1}$. For the high Q approximation, the signal will be a minimum at frequency,

$$\omega^2 = \omega_{min}^2 = \frac{1}{L_1 C_1}$$

The observed signal will be a maximum at frequency,

$$\omega^2 = \omega_{max}^2 = \frac{1}{L_1}\left(\frac{1}{2C_0 + C_2 + C_3} + \frac{1}{C_1}\right)$$

The electromechanical coupling β is defined as

$$\beta = \frac{C_1}{C_2}$$

The inverse of this is sometimes called the capacitance ratio or the piezoelectric ratio.* β can be calculated from the above equations if ω_{min}^2, ω_{max}^2, C_0, C_2, and C_3 are known. The result is,

$$\beta = \frac{2C_0 + C_3 + C_2}{C_2}\left(\frac{\omega_{max}^2}{\omega_{min}^2} - 1\right)$$

ω_{min} and ω_{max} were measured with the frequency counter at the minimum and maximum signals. C_2 was measured in the following way. When the oscillator was set at a frequency away from resonance, the impedance Z was due essentially to $2C_0 + C_3 + C_2$. The signal amplitude on the oscilloscope was recorded. The capacitance box was removed from the coaxial line at A, figure 2. A capacitor was attached to the box in place of the coax and found to give the same signal amplitude. The capacitance of the capacitor and its connector was measured with a bridge. It was 80 pf. Therefore $C_2 + C_3$ = 80pf, C_2 = 57 pf.

---

* Cady, Walter G., Piezoelectricity, p 353.

The resonances of the crystal were observed from 100 khz to 5 Mhz. The resonance near 200 khz had changes of impedance much larger than any of the other resonances. The table shows the results of measurements and calculations for this resonance. At liquid nitrogen and liquid helium temperatures $\beta = 10^{-3}$. R_1 and R_2 can be estimated from this data.

At $\omega = \omega_{min}$

$$Z \approx R_1 \approx 70\Omega$$

At $\omega = \omega_{max}$

$$\frac{1}{Z} \approx R_2 \omega^2 C_2^2 + \frac{R_1}{R_1^2 + \frac{1}{\omega^2 (2C_0 + C_2 + C_3)^2}}$$

$$\Rightarrow R_2 \approx 500\Omega$$

The Q of this mode of the crystal and its mount is then

$$Q = \frac{1}{\omega C_1} \frac{1}{R_1 + R_2} \approx 25,000$$

The Q of the resonance was also measured at liquid helium temperature by sweeping the oscillator quickly through the resonance and recording the transient response with a memory oscilloscope. The result was about 30,000.

The previous experimental results will now be compared to theory. The planar coupling constant for a piezoelectric disc is given by*

$$\beta = k_p^2 = \frac{2 d_{31}^2}{\varepsilon_{33}^T \left(s_{11}^E + s_{12}^E \right)} \qquad \text{(rationalized MKS)}$$

From room temperature data on $LiNbO_3$ provided by Crystal Technology Incorporated,

$d_{31} = .085 \times 10^{-11}$ C/N

$\varepsilon_{33}^T = .254 \times 10^{-9}$ F/m

$s_{11}^E = 5.83 \times 10^{-12}$ m^2/N

$s_{12}^E = -1.15 \times 10^{-12}$ m^2/N

Thus, $k_p^2 = \beta = 1.22 \times 10^{-3}$

This agrees with the room temperature measurement of 1.2×10^{-3} for the coupling. At liquid nitrogen and helium temperatures the coupling was 1.0×10^{-3}. It is not clear if this difference is due to error in the technique or real change in the coupling. However, for most practical purposes one may conclude that the coupling does not change significantly from room temperature down to cryogenic temperature.

---

*IRE Standards on Piezoelectric Crystals: Measurements of Piezoelectric Ceramics, 1961. This standard is reprinted in the following book, Piezoelectric Ceramics, Jaffe, B., Cook, W. C., and Jaffe, H., Academic Press, New York, 1971, See page 291 for equation for k_p^2.

The previous planar coupling constant is for the radial mode of the disc. To ensure that this mode was actually observed, the expected resonant frequency* was calculated from the known properties of the lithium niobate crystal. The result is 208 khz which agrees reasonably with the observed frequency of 196 khz at room temperature.

*Jaffe, Cook, and Jaffe, p. 32

TABLE OF RESULTS

Temp.	Pressure (μ Hg)	Signal In (vpp)	Signal Out (mvpp)	Frequency (hertz ± 1 to 2 hz)	|Z| (ohms)	β
room temp.	400 air	6.0	2.3 ± .1 off res. 30 ± 2 maximum .10 ± .02 minimum	193,000 195,942 195,864	8,700 110,000 370	1.2×10^{-3}
Liquid Nitrogen	130 air	6.0	2.5 ± .1 off res. 84 ± 4 maximum .02 ± .01 minimum	195,000 199,031 198,964	9,300 310,000 70	1.0×10^{-3}
Liquid Helium	20 He	6.0	2.5 ± .1 off res. 76 ± 4 maximum .02 ± .01 minimum	202,000 199,137 199,070	9,300 280,000 70	1.0×10^{-3}

$$\beta = \frac{86 \text{ pf}}{57 \text{ pf}} \left(\frac{f^2_{max}}{f^2_{min}} - 1 \right)$$

$$|Z| = \frac{\text{signal out}}{2.5 \text{ mvpp}} \; 9.3 \text{ k}\Omega$$

$$9{,}300\ \Omega = \frac{1}{86 \text{ pf } 2\pi \; 199{,}000 \text{ hz}}$$

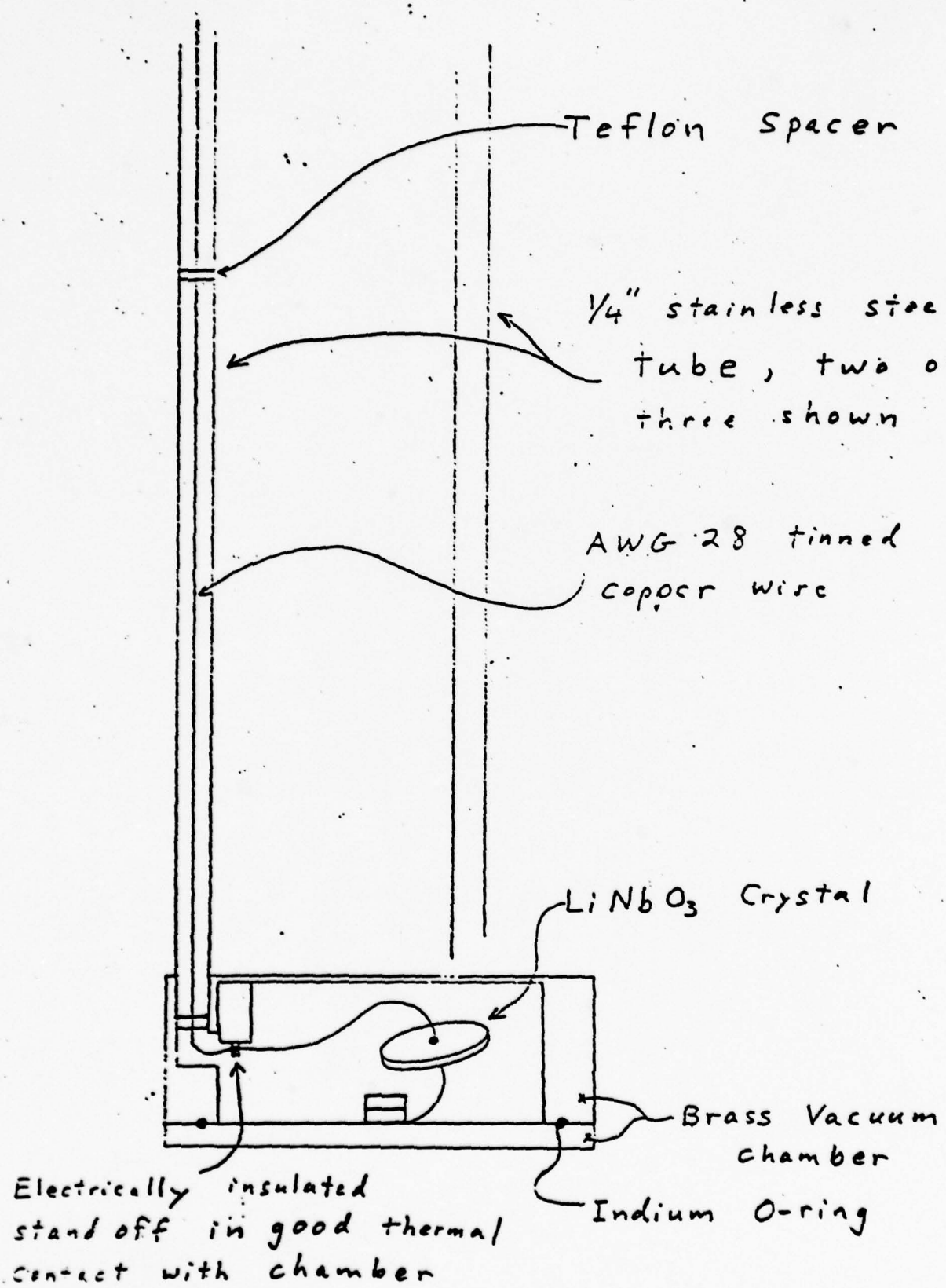

Figure 1

Scale 1:1

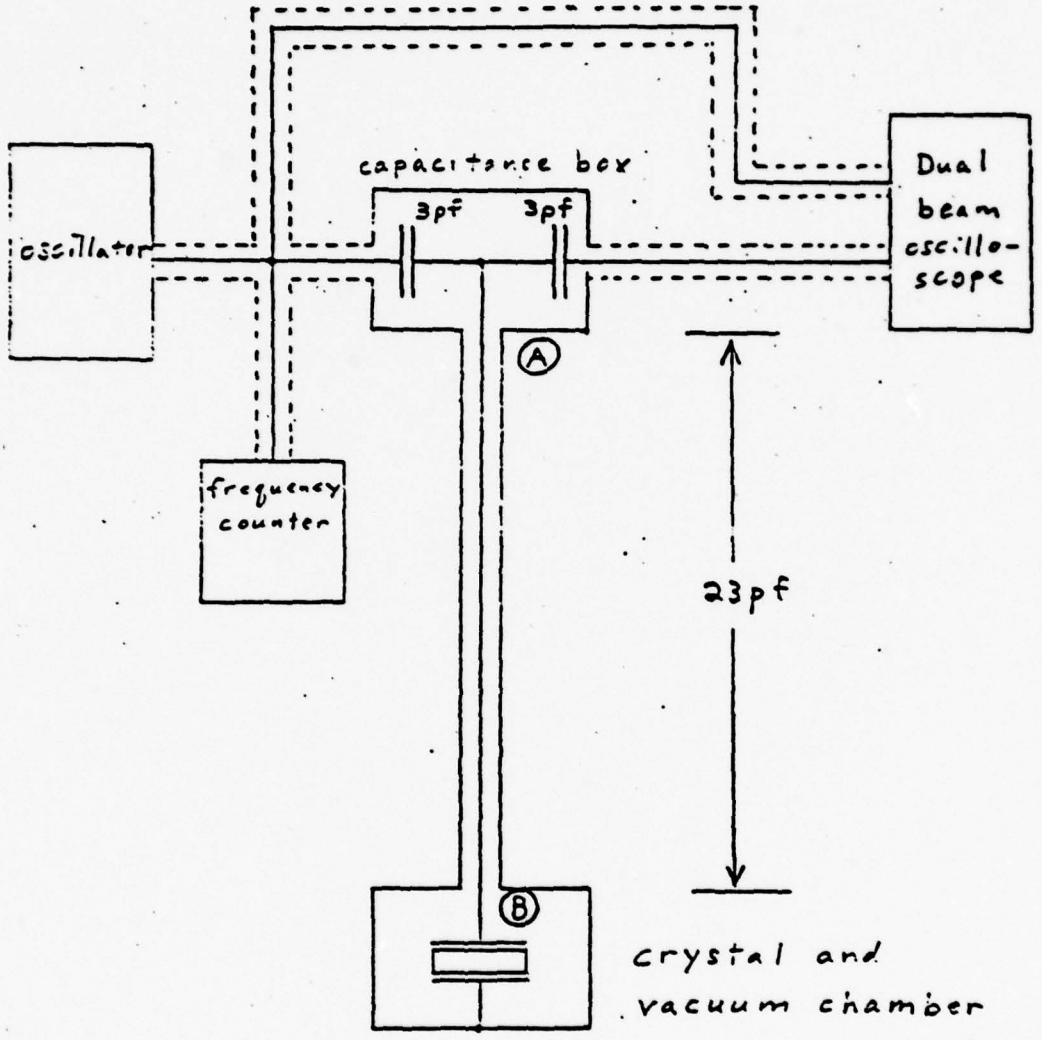
capacitance box
3pf
3pf
oscillator
Dual beam oscillo-scope
A
frequency counter
23pf
B
crystal and vacuum chamber

Figure 2

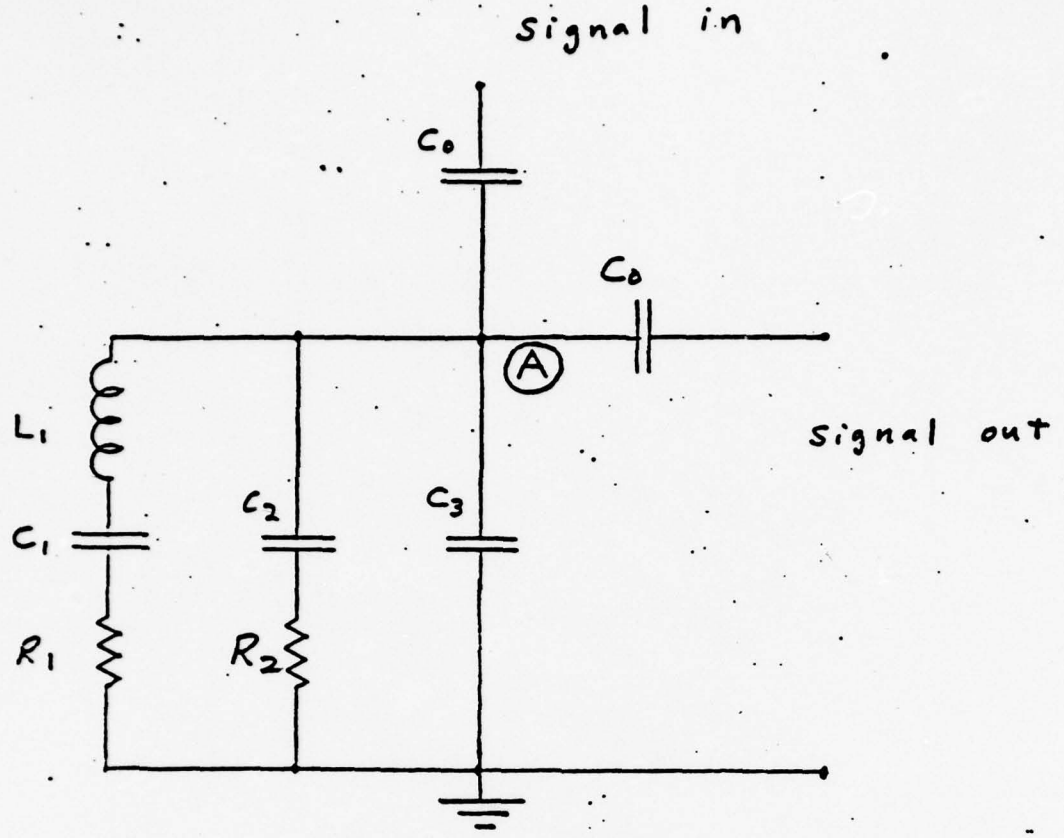

C_1, capacitance due to mechanical elasticity of mode

C_2, capacitance due to crystal dielectric constant and geometry, 57pf

C_3, capacitance of coaxial transmission line, 23pf

C_0, silver-mica capacitor, 3pf

Figure 3

LARGE 20 mK CRYOSTAT

Figures 8, 9, 10, and 11 show a cryostat which is designed to cool a 15 kg silicon crystal to 20 mK and maintain it there.

The cryostat is presently under construction at the Gravity Research Building located just off the University of Maryland campus in a relatively quiet and isolated environment. This laboratory already contains a working closed cycle liquid helium system, consisting of a CTI model 1400 liquifier, associated compressors, and a helium storage tank. The system contains enough gas to fill an appropriately sized dewar with about 200 liters of liquid helium. With this system we can produce a large 4.2 Kelvin environment. To produce millikelvin temperatures we are presently modifying a large vacuum chamber and dewar to accept a SHE DRI-423 helium dilution refrigerator which is expected to be delivered early in 1979.

A description of the present design of the cryostat will now be given. The cryostat is suspended inside a large vacuum chamber, 10 feet long by 8 feet in diameter. The copper vapor shield hangs from the inside top of the chamber through acoustic isolation filters. Boil off liquid helium vapor from the dewar circulates through copper tubing soldered to the vapor shield, thus cooling it. This shield is covered with several layers of aluminum coated mylar and nylon net (superinsulation) for radiation shielding. The liquid helium dewar is enclosed by the vapor shield, but hangs from its own acoustic isolation filters attached to the vacuum chamber, as shown in the figures. The stainless steel dewar is connected to the isolation via a dacron strap. The thermal conduction down this strap is expected to be the main heat leak into the dewar. If the upper end of the strap is thermally shorted to the vapor shield then the expected boil off rate is 12 liters per day out of a total of 200 liters in the dewar. The dewar's outside and inside surfaces are covered with 1/16 inch copper shells to provide uniform temperature. Covering the outer copper shell is several

layers of superinsulation. Inside the dewar is a copper shield to be maintained at 1.3 Kelvin by the cold plate of the dilution refrigerator. Rods made of nylon or vespel SP-22 (Dupont graphite filled polyimide resin) provide the necessary support of the 1.3 Kelvin shield and thermal isolation from the 4.2 Kelvin copper shell of the dewar. Inside the 1.3 Kelvin shield are tracks upon which a cart supporting the rest of the experiment can be rolled in and out. As shown in figures 9 and 10, acoustic isolation filters (alternating layers of felt and steel) sit on the cart. These filters support a platform which is also maintained at 1.3 Kelvin. The 15 kg silicon crystal is coated with niobium and supported inside a 20 mK copper shield by magnetic levitation. The latter requires superconducting coils with persistent currents mounted inside the 20 mK shield. This shield rests on a ring suspension which is supported on the 1.3 K platform by vespel rods. A strong thermal link is made from the ring suspension to the mixing chamber of the dilution refrigerator with an extremely pure copper braid. The expected heat flow from the 1.3 K platform to the 20 mK ring suspension through the vespel rods is about 3 microwatts. Other expected sources of heat leak are less than ½ microwatt. The dilution refrigerator can maintain the experiment at 20 mK with a heat leak of 3½ microwatts with a 2 mK temperature drop along the copper braid. This assumes that the heat generated by the persistent current in the coils, eg., from flux jumps, is smaller than the heat leak. Further design and research might be needed to ensure this.

There are two separate vacuums in the cryostat. The space between the vacuum chamber, the vapor shield, and the dewar is kept evacuated with a diffusion pump. This space contains the superinsulation which needs a good vacuum to be effective. The 4.2 Kelvin copper shell inside the dewar is the second vacuum space. It has its own pumpout line. The 1.3 Kelvin and 20

millikelvin shields are not vacuum tight. During cooldown several microns of pressure of helium will be left in this space to allow cooling of everything by conduction. At 4.2 Kelvin this gas is pumped out and further cooling is accomplished by the dilution refrigerator. The levitation coils are not turned on until the crystal has been cooled to 20 mK. The crystal has to be levitated slowly to ensure that the changing magnetic field does not heat it up.

The dilution refrigerator must be supplied with liquid helium (He^4). Liquid helium is consumed to precool the He^3 returning to the refrigerator. Liquid helium is also consumed by the 1.3 Kelvin coldplate. Therefore a separate liquid helium container is built onto one of the copper shells of the dewar. There is a thermal link (such as a thick copper braid) between the cold plate and the 1.3 Kelvin copper shield and platform.

The following pages outline the thermal calculations for the 1.3 Kelvin and 20 millikelvin shields.

I. 1.3 K shield heat balance

A. Heat flow into shield from 4.2 K to 1.3 K

1. Conduction through < 10^{-7} torr He gas;
$\dot{q}$ < .7 mW

2. Black body radiation;
$\dot{q}$ = .16 mW

3. Conduction through 10 niobium wires, 4 mils (102 microns) in diameter and 300 cm long;
$\dot{q}$ = .05 mW

4. Conduction through 7 support rods, ½ inch (1.27 cm) diameter, 1 inch (2.54 cm) long;
nylon $\dot{q}$ = 1.6 mW
vespel SP-22 $\dot{q}$ = 1.4 mW

B. Heat flow out of shield due to 1.3 K cold plate of dilution refrigerator; up to 20 mW

C. Conclusion, the excess cooling power of the cold plate is more than enough to take care of the above sources of heat.

D. The thermal gradient across the copper shield from the supports to the cold plate;

nylon ΔT = 2.8 mK

vespel ΔT = 2.4 mK

II. 20 mK shield heat balance

A. Heat flow into shield from 1.3 K to 20 mK

1. Conduction through < 10^{-10} torr He gas;
$\dot{q}$ < .04 μW

2. Black body radiation
$\dot{q}$ = .18 μW

3. Conduction through 8 niobium wires, 4 mils, (102 microns) in diameter and one meter long;
$\dot{q}$ = .12 μW

4. Conduction through 4 vespel supports, .25 inches (6.4 mm) diameter, 2 inches (51 mm) long; $\dot{q}$ = 3.1 μW

B. Heat flow out of 20 mK shield to dilution refrigerator after the system has been cooled; when the refrigerator is at 18 mK, its cooling power is 3½ microwatts.

C. Net heat flow; the dilution refrigerator can maintain the experiment at 20 mK with an expected heat leak of about 3½ microwatts with a 2 mK temperature drop along the copper braid heat link. This assumes that the heat generated by magnetic levitation is small.

D. The thermal gradient across the 20 mK shield is expected to be less than 1 μK.

III. Cooldown time; the 15 kg silicon crystal, the copper shield, and the ring suspension can be cooled from 1.3 K to 20 mK in less than one day.

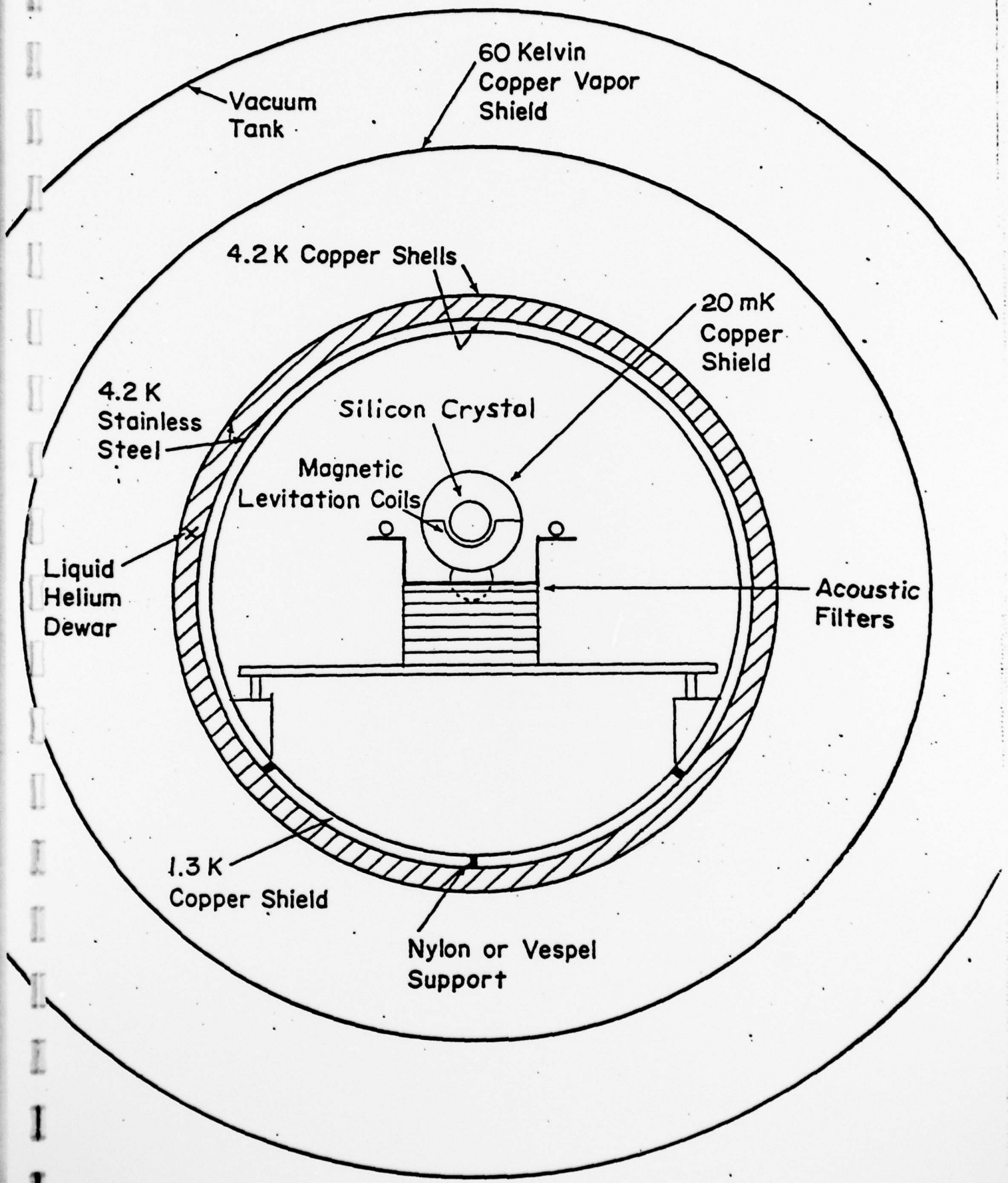
60 Kelvin
Copper Vapor
Shield
Vacuum
Tank
4.2 K Copper Shells
20 mK
Copper
Shield
4.2 K
Stainless
Steel
Silicon Crystal
Magnetic
Levitation Coils
Liquid
Helium
Dewar
Acoustic
Filters
1.3 K
Copper Shield
Nylon or Vespel
Support

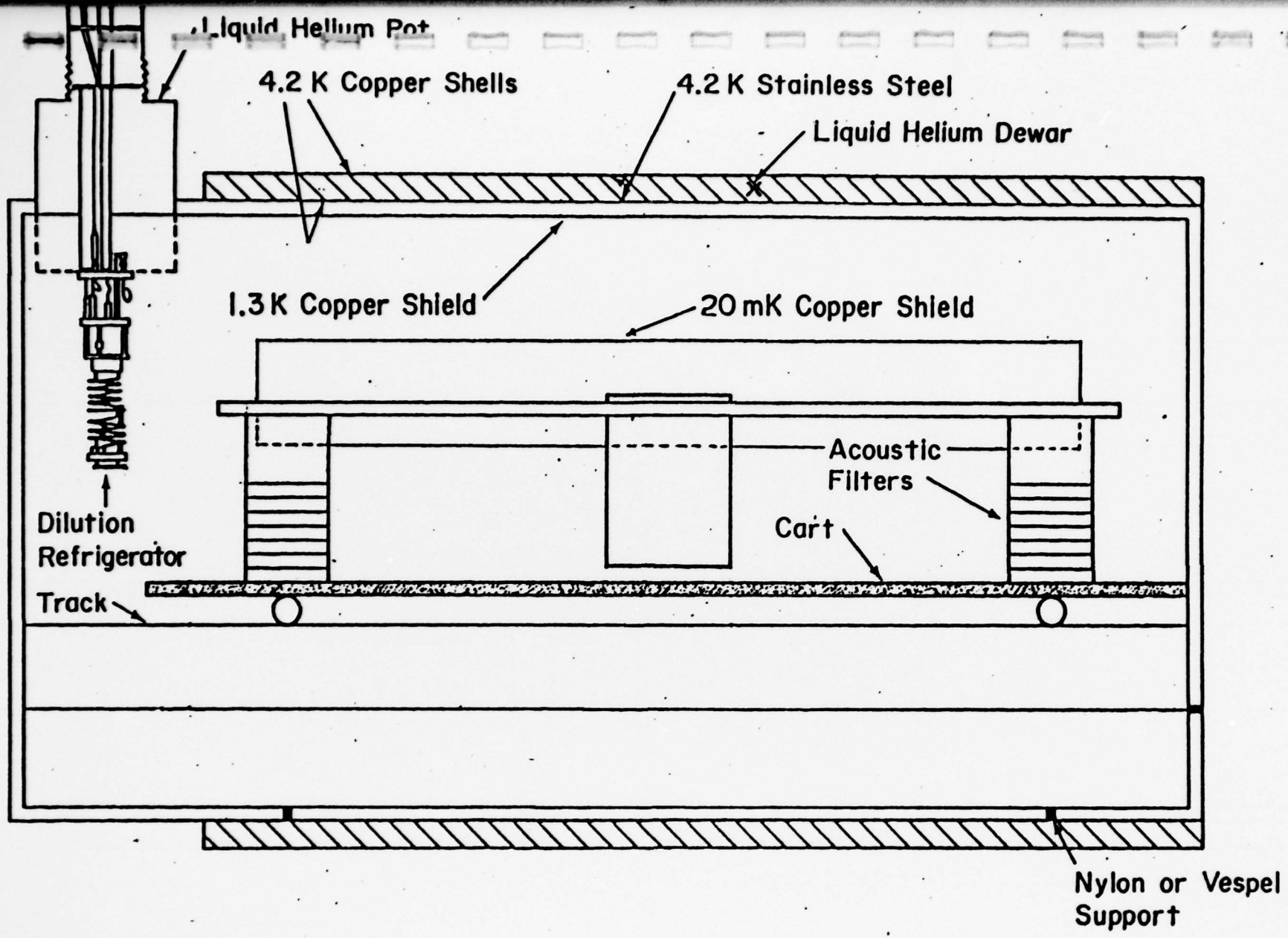

Not Shown: Thermal Links to Dilution Refrigerator

Bar and Suspension Inside 20 mK Shield

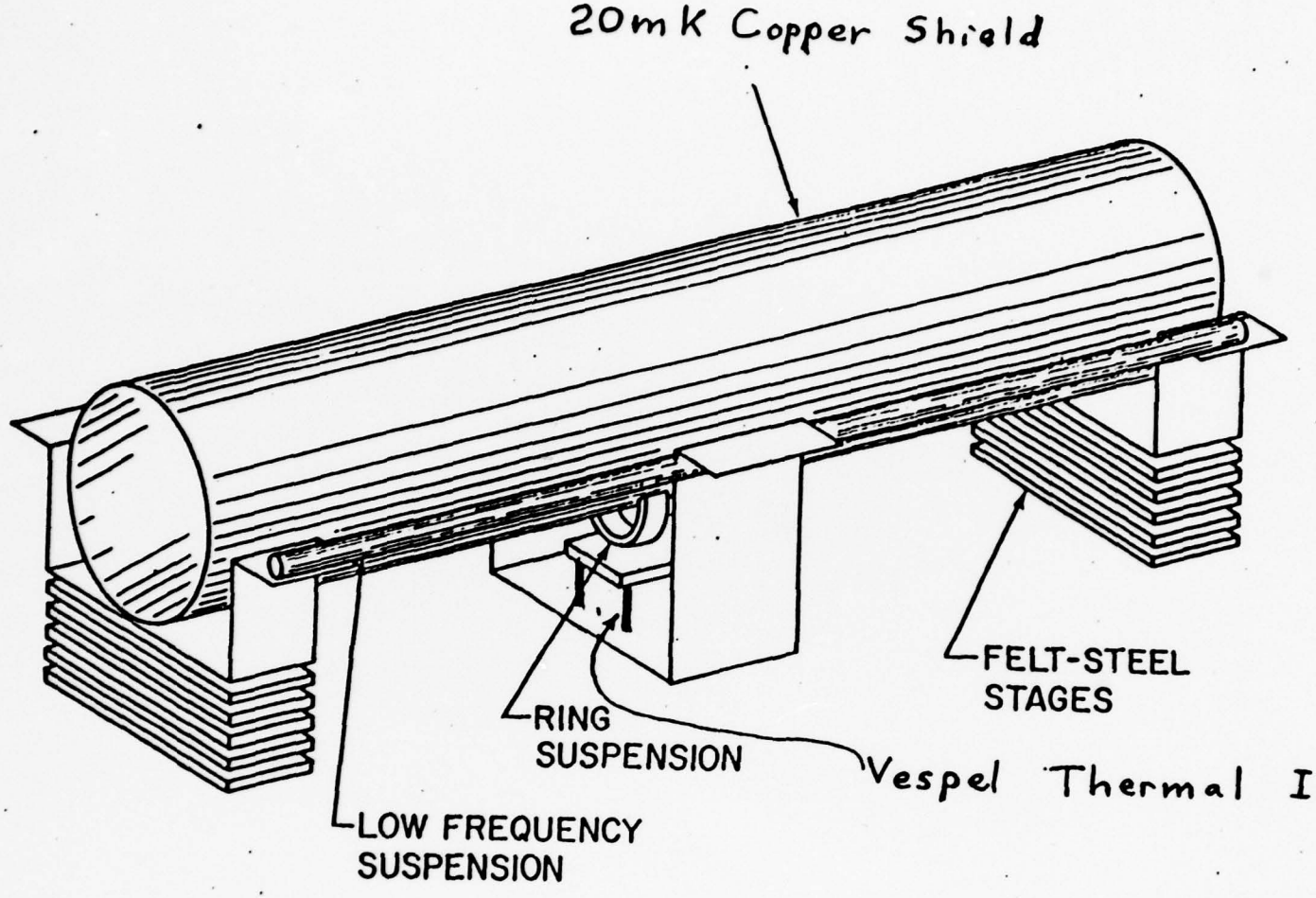
20mK Copper Shield
FELT-STEEL
STAGES
RING
SUSPENSION
Vespel Thermal Isolation
LOW FREQUENCY
SUSPENSION

BY
CHKD BY
DATE
SUBJECT m'K CRYOSTAT
SHEET NO. OF
JOB NO.

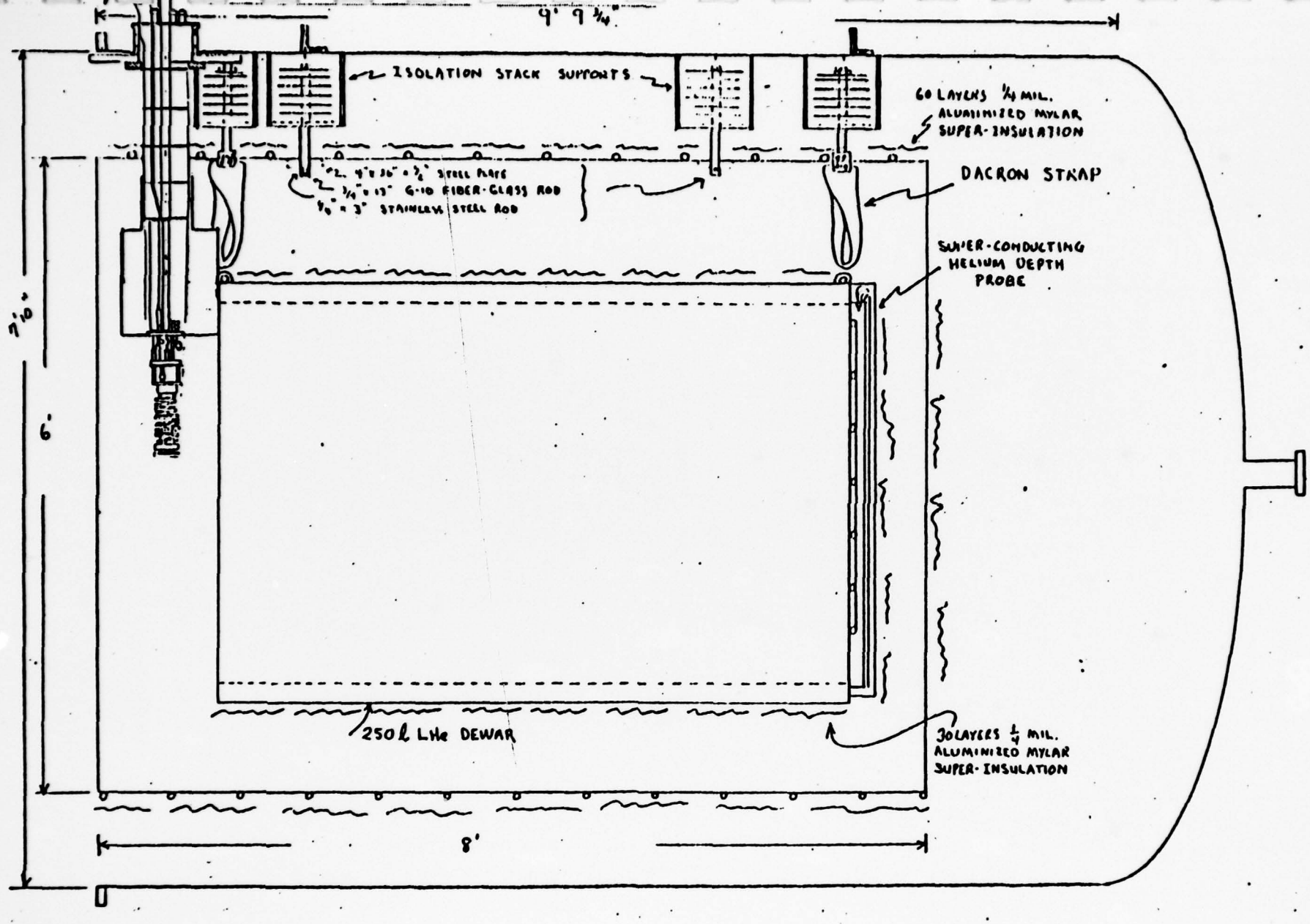

70

SENSITIVITY OF A GRAVITATIONAL GRADIOMETER USING AN ELASTIC SOLID

As in most other measurements, there is a continuous background of signals resulting from interaction of an elastic solid gradiometer with its heat bath, electronics, cosmic radiation, seismic noise, cryogenics, ... Fluctuations in this background may resemble any kind of signal. Criteria, ultimately based on the theory of probability are established to enable decisions to be made, at a certain level of confidence, that observed signals originate in sources outside of the gradiometer.

In Figure 1 is shown the external signal V_G which may have any time dependence whatsoever, together will all relevant internal noise sources. V_e and I_e are voltage and current noise sources selected to account for all noise generated in the amplifier following terminals xx . V_1 is a voltage noise source describing most of the thermal fluctuations of the oylinder mode, I_2 is a current noise source accounting for the noise of resistance R_2 which couples the heat bath to output capacity C_2 and the cylinder mode. The amplifier is followed by a demodulator and low pass filter. The Maxwell network relations together with integrals over the filter bandpass then lead to expressions for the signal and noise power outputs, for any given type of signal.

Fluctuations

The design of the demodulator and low pass filter will depend on the dynamical variables chosen to specify the state of the cylinder. Let us therefore consider first the available amplifier output voltage. This may be written in terms of the fluctuating amplitude $A(t)$, fluctuating phase $\varphi(t)$ and mode angular frequency ω_o , as

$$V(t) = A(t) \sin(\omega_o t + \varphi(t)) \qquad (1)$$

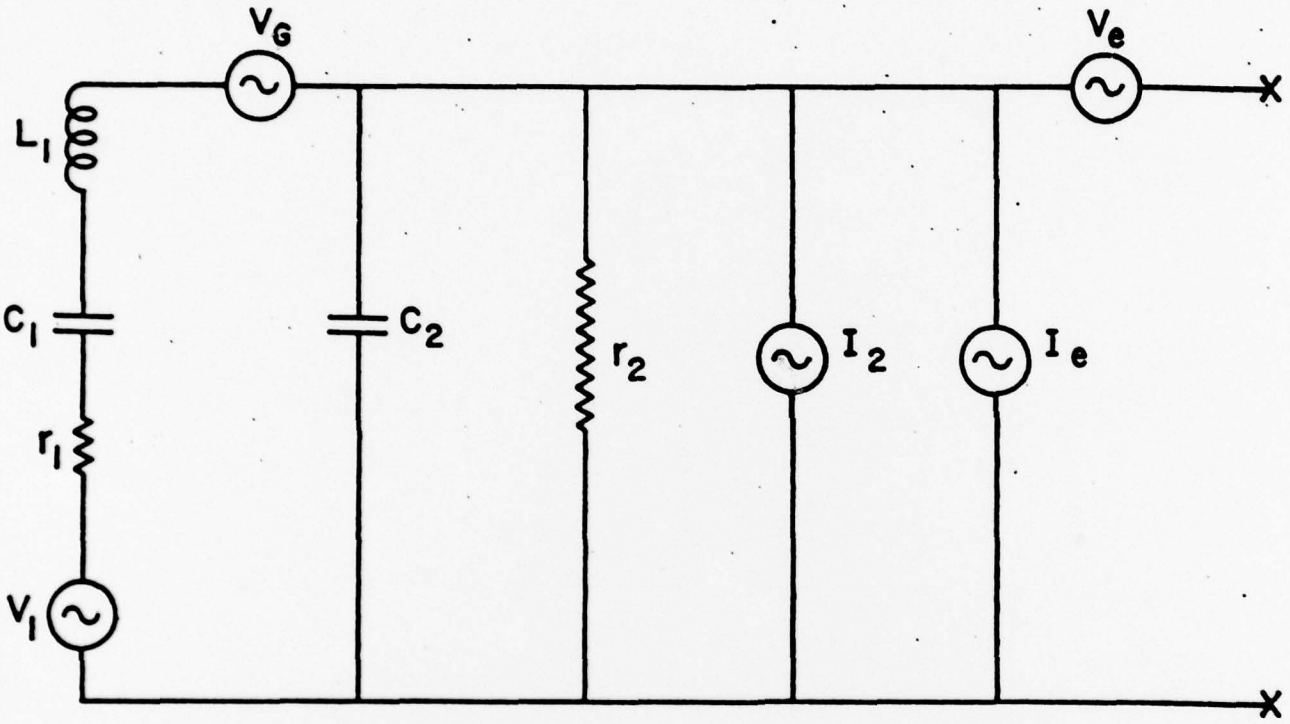

FIGURE 1

We choose variables x and y defined by

$$x = A\cos\varphi \tag{2}$$

$$y = A\sin\varphi \tag{3}$$

to describe the cylinder state and its time evolution. (2) and (3) are obtained from (1) by means of electronic devices which multiply (1) by $\cos\omega_0 t$ and separately by $\sin\omega_0 t$, from a quartz oscillator tuned as closely as possible to ω_0. The separate channels then process x and y. This multiplication gives for one channel

$$2V(t)\cos\omega_0 t = A\sin\varphi + A\sin(2\omega_0 t + \varphi) \tag{4}$$

and for the other channel

$$2V(t)\sin\omega_0 t = A\cos\varphi - A\cos(2\omega_0 t + \varphi) \tag{5}$$

(4) and (5) are then coupled to low pass filters which remove the terms containing frequencies $2\omega_0$ and give time averages.

$$\bar{x}(t) = \frac{1}{\tau}\int_t^{t+\tau} A(t)\cos\varphi(t)\,dt \tag{6}$$

$$\bar{y}(t) = \frac{1}{\tau}\int_t^{t+\tau} A(t)\sin\varphi(t)\,dt \tag{7}$$

The state of the harmonic oscillator representing the cylinder mode is then represented by a point in the $\bar{x}$, $\bar{y}$ plane. This point undergoes a kind of random walk as the system evolves.

Short Pulse Algorithm

Let us assume that a short pulse of gravitational gradient may produce a sudden displacement of the point x, y in any direction whatsoever with equal probability. To compute the sensitivity we calculate the expected changes $\Delta\bar{x}$ and $\Delta\bar{y}$ which may be produced by the background noise.

The power spectra of the noise voltage V_1 and noise current I_2 are given by

$$P_{V1} = \frac{2\hbar\omega R_1(\omega)}{\pi\left(e^{\hbar\omega/kT}-1\right)} \approx \frac{2kT R_1(\omega)}{\pi} \qquad (8)$$

$$P_{I2} = \frac{2\hbar\omega}{\pi R_2(\omega)\left(e^{\hbar\omega/kT}-1\right)} \approx \frac{2kT}{\pi R_2(\omega)} \qquad (9)$$

On the far right of (8) and (9) are the limits for $\frac{\hbar\omega}{kT} << 1$. Let the power spectra of the electronics current and voltage noise sources be P_{Ie} and P_{Ve} respectively. These sources may be somewhat correlated. A low pass Butterworth filter is assumed to be employed after demodulation, with upper cut off angular frequency ω_v, averaging time τ_{obs} and power response $\left(1+\frac{\omega}{\omega_v}\right)^{-4}$. It is also assumed that Q_1 and Q_2 defined by $Q_1 = \frac{\omega L_1}{R_1}$, $Q_2 = \omega C_2 R_2$ are both $>> 1$. To good approximation the quantity $\langle(\Delta\bar{x})^2+(\Delta\bar{y})^2\rangle$ may then be computed as

$$\langle(\Delta\bar{x})^2+(\Delta\bar{y})^2\rangle = \left\langle\left(\frac{d\bar{x}}{dt}\right)^2+\left(\frac{d\bar{y}}{dt}\right)^2\right\rangle \tau^2 \qquad (10)$$

and

$$\left\langle \left(\frac{d\bar{x}}{dt}\right)^2 + \left(\frac{d\bar{q}}{dt}\right)^2 \right\rangle \tau^2 = \int_{-\infty}^{\infty} \frac{\omega^2\tau^2 \left(P_{Ve} + \left[P_{I2} + P_{Ie} \right]/\omega^2 C_2^2 \right) d\omega}{\left(1 + \frac{\omega}{\omega_0}\right)^4}$$

$$+ \frac{2}{\pi\omega_0 Q_1 C_2^2} \int_{-\infty}^{\infty} \frac{\omega^2\tau^2}{\left(1 + \frac{\omega}{\omega_0}\right)^4 \left(\left(\frac{\omega_0}{Q_1}\right)^2 + 4\omega^2 \right)} \left[\frac{kT}{L_1} + \frac{\pi P_{Ie}}{2L_1 R_1 \omega_0^2 C_2^2} \right] d\omega \qquad (11)$$

The first integral on the right of (11) gives the wideband contribution, and the second integral gives the narrow band contribution. The first term in the bracket of the second integral gives the narrow band contribution of the noise sources V_1 and I_2, and the second term in the bracket gives the narrow band contribution due to the electronics current source I_e. Carrying out the integrations gives

$$\left\langle (\Delta\bar{x})^2 + (\Delta\bar{q})^2 \right\rangle = \frac{\pi^2}{B} \left[\frac{\pi\omega_0 \left(P_{Ve} + \left[P_{I2} + P_{Ie} \right]/\omega_0^2 C_2^2 \right)}{\sqrt{2}} \right. \qquad (12)$$

$$\left. + \left(\frac{kT\omega_0}{Q_1 L_1} + \frac{\pi P_{Ie}}{2L_1^2 \omega_0^2 C_2^2} \right) \frac{1}{\omega_0 \sqrt{B}\, \omega_0^2 C_2^2} \right] \qquad (13)$$

In (12) we have employed the relation:

$$\omega_0 \tau_{obs} = \frac{\pi}{\sqrt{B}}$$

for a Butterworth filter. It is illuminating to discuss the significance of the terms in (12). The first term tells us that for the wideband noise the fluctuations in the voltage amplitude are essentially the same magnitude as the noise voltage squared itself. The two terms in the narrow band noise

contribution may be written in terms of (13) and the e folding time

$\tau_{mode} = \frac{2Q_1}{\omega_0}$ as

$$\frac{\pi k T \tau_{obs}}{4 L_1 \omega_0^2 C_2^2 \tau_{mode}} \left(1 + \frac{\pi P_{Ie} \tau_{mode} C_1}{4 C_2^2 k T}\right) \qquad (14)$$

The electronic noise raises the mode temperature from T to the value $T\left(1 + \frac{\pi P_{Ie} \tau_{mode} C_1}{4 C_2^2 k T}\right)$, and the fluctuations in narrow band noise voltage are a factor $\frac{\tau_{obs}}{\tau_{mode}}$ smaller than the squared narrow band total voltage. It is also clear from (14) that reduction of the temperature T must be accompanied by improved electronics.

For these assumptions an optimal filter is one for which the low pass Butterworth filter cut off ω_0 is chosen so that (12) is an extremum. Setting the derivative of (12) with respect to ω_0 equal to zero gives $\tilde{\omega}_0$, the optimal bandwidth as

$$\tilde{\omega}_0 = \sqrt{\frac{k T \left(1 + \frac{\pi P_{Ie} \tau_{mode} C_1}{4 C_2^2 k T}\right)}{L_1 \omega^2 C_2^2 \tau_{mode} \pi \left(P_{Ve} + \frac{(P_{I2} + P_{Ie})}{\omega_0^2 C_2^2}\right)}} \qquad (15)$$

Let us define a system "temperature" by the criterion that it is the sudden change in temperature of the cylinder mode alone which will give the change equal to the mean square fluctuations computed by (12). Let this temperature be T'. We have, then

$$\frac{kT'}{4}\left(\frac{1}{\omega_1^2 C_2^2}\right) = \frac{\pi^2}{8}\left[\frac{-\tilde{\omega}_0\left[P_{Ve} + (P_{I2} + P_{Ie})/\omega_0^2 C_2^2\right]}{\sqrt{2}} + \frac{1}{\tilde{\omega}_0 \omega_0^2 C_2^2 \sqrt{8}}\left(\frac{2kT}{L_1 \tau_{mode}}\left(1 + \frac{\pi P_{Ie} \tau_{mode} C_1}{4 C_2^2 k T}\right)\right)\right] \qquad (16)$$

solving for T' and rearranging terms then gives

$$T' = T_{internal}\left[\frac{\pi \tau_{obs}}{4\tau_{mode}}\left(1+\frac{\pi P_{Ie}\tau_{mode}C_1}{4C_1^2 kT}\right)+\frac{\pi^4\left[P_{I2}+P_{Ie}+\omega_0^2 C_2^2 P_{Ve}\right]}{32\,\tau_{obs}\,(kT/L_1)}\right] \qquad (17)$$

(17) then tells us that the "effective mode temperature" is the thermodynamic temperature times the sum of a number of factors. The first factor is roughly the optimal filter averaging time divided by the mode e folding time, the second is roughly the ratio of the total equivalent squared broad band noise current divided by the total squared (narrow band) mode noise current. This analysis is applicable to any gravitational gradiometer described by the noise sources and equivalent circuit of Figure 1.

Coupling and Quality Factor

Expression (17) stresses the importance of a high quality factor for an elastic solid sensor. (17) also makes clear the importance of having the largest possible coupling (small L_1) together with electronics with small current and voltage noise.

A 1400 kilogram aluminum cylinder, which is carefully mounted, may have $Q \rightarrow 500{,}000$ at room temperature, with no crystals or other attached instrumentation. Very recently we installed a number of PZT-8 (lead zirconate titanate) crystals on an aluminum cylinder having a diameter close to one meter and length 155 centimeters, of mass 3400 kilograms, at room temperature. The loaded Q was 150,000, $C_2 = 3650 \times 10^{-12}$ farads, $C_1 = 2 \times 10^{-12}$ farads, $L_1 = 5{,}000$ Henries $r_1 = 331\ \Omega$, $r_2 = 8 \times 10^6\ \Omega$. At lower temperatures Professor J.-P. Richard and Dr. Wm. Davis obtained loaded $Q \rightarrow 10^6$ for an aluminum cylinder with a parametric capacitor. Dr. Suzuki, Dr. Tsubono and Dr. Hirakawa have observed much higher Q's with type 5056 aluminum at low temperatures.

Publications During the Past Year

J. P. Richard, "Monocrystals for the Investigation of Gravity Phenomena" Invited Paper to the 5th International Symposium on Space Relativity, Dubrovnik, Yugoslavia, October 5, 1978.

J. Weber, "Gravitational Radiation", to be published in Einstein 100th Anniversary Book.

J. Weber, "Gravitational Waves", to be published in Einstein 100th Anniversary Book.

J. Weber, "The Search for Gravitational Radiation", to be published in Einstein 100th Anniversary Book.